

**UNIVERSITY OF STRATHCLYDE**

**THE DEPARTMENT OF BIOMEDICAL  
ENGINEERING**

**Master of Science  
Dissertation**

---

**Characterisation of an expandable valve  
testing apparatus for the development of  
growth compensating paediatric heart  
valves.**

**Author: Vendula Pavlikova**

**Supervisors: Prof. Terrence Gourlay**

**Dr. Monica Rozeik**

**Glasgow, 2015**

## Declaration

This thesis is the result of the author's original research. It has been composed by the author and has not been previously submitted for examination which has led to the award of a degree.

The copyright of this thesis belongs to the author under the terms of the United Kingdom Copyright Acts as qualified by University of Strathclyde Regulation 3.50. Due acknowledgement must always be made of the use of any material contained in, or derived from, this thesis.

Signed:

Date:

## Acknowledgements

This project would have not been possible without the support of many people.

Firstly I would like to thank to my supervisors, Prof. Terence Gourlay and Dr. Monica Rozeik, for all their help, enthusiasm, supervision, support, knowledge and valuable guidance throughout this project. Their wisdom and insight have been much appreciated.

I would also like to express my gratitude to my family, especially to my parents and my partner, for all their patience, support and calming words when it was needed.

## Abstract

Congenital heart disease is a serious problem affecting up to 9 in every 1,000 babies born in UK. <sup>1</sup> When such a baby is born with a damaged heart valve, it can seriously affect the blood flow through the heart and the entire body. Therefore they have to undergo a life-threatening surgery to have a prosthetic aortic valve replacement. As the paediatric heart is growing, the prosthetic valve should be growing as well, but currently no expandable prosthesis yet exists. During their lifetime, the child has to undergo several serious surgeries which are a burden to them and the options are still limited. An expandable heart valve could compensate these surgeries. Instead of experiencing multiple surgeries, they could have the only one at the beginning of their life. The normal valve opens and closes approximately 103,000 times each day and a prosthetic valve needs to survive at least 200 million cycles to prove that it is durable.

The aim of this project is to design and develop an expandable holder that could be deployed in testing of a growth compensating paediatric heart valve. An important part of the project is to perform a set of tests in the heart valve tester using the expandable holder. Obtained results from the heart valve tester have been analysed and discussed as well as future considerations have been proposed.

# Contents

Declaration.....	2
Acknowledgements.....	3
Abstract.....	4
Contents.....	5
List of Figures .....	7
List of Abbreviations .....	10
1. Literature Review.....	11
1.1. The Anatomy of Heart.....	11
1.2. Blood Circulation.....	12
1.3. Cardiac Cycle .....	14
1.4. The Heart Valves .....	15
1.4.1. Anatomy of the Heart Valve .....	15
1.4.2. Fluid Dynamics of the Valves .....	16
1.5. Congenital Heart Diseases .....	17
1.6. Treatment strategies for Paediatrics .....	19
2. Aims and Objectives.....	22
3. Methodology.....	24
3.1. Introduction .....	24
3.2. Design.....	24
3.2.1. Design Specifications.....	24
3.2.2. Design Ideas .....	25
3.2.3. Design Concept .....	26
3.3. Experimentation.....	27
3.3.1. Pulse Duplicator .....	28
3.3.2. Valve Attachment .....	30
3.3.3. Testing.....	31
3.3.3.1. Valve not in place.....	32
3.3.3.2. The CoreValve testing .....	32
3.3.3.3. Iris mechanism without/with the CoreValve .....	33
4. Results.....	36
4.1. Valve not in place.....	36

4.2.	The CoreValve testing .....	42
4.3.	Iris mechanism .....	47
4.3.1.	Iris mechanism without the CoreValve.....	47
4.3.2.	Iris mechanism with valve.....	52
5.	Discussion.....	56
5.1.	Valve not in place.....	56
5.2.	The CoreValve testing .....	56
5.3.	Iris mechanism .....	57
5.3.1.	Iris without the CoreValve .....	57
5.3.2.	Iris with the CoreValve .....	58
6.	Future perspectives .....	60
6.1.	Material.....	60
6.2.	Shape of the Iris .....	60
6.3.	Automated mechanism.....	61
7.	Conclusion.....	62
8.	References .....	63

## List of Figures

Figure 1: (a) Location of the heart in the body. <sup>3</sup> (b) Anatomy of the heart. <sup>4</sup> .....	11
Figure 2: Circulatory system of blood in the body. <sup>9</sup> .....	13
Figure 3: Distribution of valves in the heart. <sup>12</sup> .....	16
Figure 4: Papillary muscles and chordae tendinae. <sup>13</sup> .....	16
Figure 5: Normal Aortic Valve on the left side, Bicuspid Aortic Valve on the right side. <sup>18</sup> ...	19
Figure 6: Melody valve. <sup>20</sup> .....	20
Figure 7: Iris mechanism idea, 3D printed parts. ....	27
Figure 8: Testing device. ....	27
Figure 9: Pulse duplicator – pumping system. ....	28
Figure 10: Pulse duplicator – testing system. ....	28
Figure 11: CoreValve, heart valve used for testing: (a) top view. (b) front view. ....	30
Figure 12: Valve attachment: (a) a holder with silicon mould, (b) the heart valve placed onto the holder. ....	31
Figure 13: CoreValve placed in Pulse Duplicator. ....	33
Figure 14: Valve attached to a holder: (a) side view, (b) bottom view. ....	33
Figure 15: Iris mechanism placed in Pulse Duplicator: (a) bottom view 22 mm annulus, (b) bottom view 16 mm annulus. ....	34
Figure 16: CoreValve placed onto Iris mechanism in Pulse Duplicator. ....	34
Figure 17: CoreValve placed onto Iris mechanism. ....	35
Figure 18: No valve in place – TPG of second cycle measured at 40 bmp, 33 mm diameter. ....	37
Figure 19: No valve in place – TPG of second cycle measured at 70 bmp, 33 mm diameter. ....	37
Figure 20: No valve in place – TPG of third cycle measured at 104 bmp, 33 mm diameter. ....	38
Figure 21: No valve in place – TPG of third cycle measured at 40 bmp, 25 mm diameter. ..	38
Figure 22: No valve in place – TPG of third cycle measured at 70 bmp, 25 mm diameter. ..	39
Figure 23: No valve in place – TPG of eighth cycle measured at 104 bmp, 25 mm diameter. ....	39
Figure 24: No valve in place - average TPG values represented for 33 mm diameter in bar chart with error bars. ....	40
Figure 25: No valve in place - average TPG values represented for 31 mm diameter in bar chart with error bars. ....	41
Figure 26: No valve in place - average TPG values represented for 27 mm diameter in bar chart with error bars. ....	41
Figure 27: No valve in place - average TPG values represented for 33 mm diameter in bar chart with error bars. ....	42
Figure 28: Valve in place – TPG of second cycle measured at 40 bmp, 23 mm diameter. ....	43
Figure 29: Valve in place – TPG of third cycle measured at 70 bmp, 23 mm diameter. ....	43
Figure 30: Valve in place – TPG of tenth cycle measured at 104 bmp, 23 mm diameter. ....	44
Figure 31: Valve in place – TPG of second cycle measured at 40 bmp, 16 mm diameter. ....	44
Figure 32: Valve in place – TPG of second cycle measured at 70 bmp, 16 mm diameter. ....	45
Figure 33: Valve in place – TPG of third cycle measured at 104 bmp, 16 mm diameter. ....	45

Figure 34: Valve in place - average TPG values represented for 23 mm diameter in bar chart with error bars. ....	46
Figure 35: Valve in place - average TPG values represented for 20 mm diameter in bar chart with error bars. ....	47
Figure 36: Valve in place - average TPG values represented for 16 mm diameter in bar chart with error bars. ....	47
Figure 37: Iris mechanism without the CoreValve – TPG of second cycle measured at 40 bmp, 22 mm diameter. ....	48
Figure 38: Iris mechanism without the CoreValve – TPG of third cycle measured at 70 bmp, 22 mm diameter. ....	48
Figure 39: Iris mechanism without the CoreValve – TPG of fourth cycle measured at 104 bmp, 22 mm diameter. ....	49
Figure 40: Iris mechanism without the CoreValve – TPG of second cycle measured at 40 bmp, 16 mm diameter. ....	49
Figure 41: Iris mechanism without the CoreValve – TPG of second cycle measured at 70 bmp, 16 mm diameter. ....	50
Figure 42: Iris mechanism without the CoreValve – TPG of second cycle measured at 104 bmp, 16 mm diameter. ....	50
Figure 43: Iris mechanism without the CoreValve - average TPG values represented for 22 mm diameter in bar chart with error bars. ....	51
Figure 44: Iris mechanism without the CoreValve - average TPG values represented for 16 mm diameter in bar chart with error bars. ....	52
Figure 45: A Iris mechanism without the CoreValve - average TPG values represented for 9 mm diameter in bar chart with error bars. ....	52
Figure 46: Iris mechanism with the CoreValve – TPG of third cycle measured at 40 bmp, 22 mm diameter. ....	53
Figure 47: Iris mechanism with the CoreValve – TPG of third cycle measured at 70 bmp, 22 mm diameter. ....	53
Figure 48: Iris mechanism with the CoreValve – TPG of third cycle measured at 104 bmp, 22 mm diameter. ....	54
Figure 49: Iris mechanism with the CoreValve - average TPG values represented for 22 mm diameter in bar chart with error bars. ....	55
Figure 50: The TPG difference of the CoreVavle in the Iris and the Iris alone, 22 mm diameter. ....	55
Figure 51: Mechanism of Shutter. An idea for an expandable holder. <sup>31</sup> .....	61



## List of Tables

Table 1: Design ideas. ....	25
Table 2: Parameters obtained from testing apparatus.....	30
Table 3: No valve in place - average $\pm$ standard error of the mean (SEM) of 3 maximal values of TPG, (a) 33 and 31 mm diameters, (b) 27 and 25 mm diameters. ....	40
Table 4: Valve in place - average $\pm$ standard error of the mean (SEM) of 3 maximal values of TPG, (a) 23 and 20 mm diameters, (b) 16 mm diameter. ....	46
Table 5: Iris mechanism without the CoreValve - average $\pm$ standard error of the mean (SEM) of 3 maximal values of TPG, (a) 22 and 16 mm diameters, (b) 9 mm diameter. ....	51
Table 6: Iris mechanism with the CoreValve - average $\pm$ standard error of the mean (SEM) of 3 maximal values of TPG for 22 mm diameter. ....	54

## List of Abbreviations

ABS	Acrylonitrile Butadiene Styrene
AC	Aortic Chamber
ASD	Atrial Septal Defect
AV	Atrioventricular Valve
CO	Cardiac Output
ECM	Extracellular Matrix
HR	Heart Rate
LA	Left Atrium
LV	Left Ventricle
LVC	Left Ventricular Chamber
MV	Mitral Valve
PBS	Phosphate Buffered Saline
RA	Right Atrium
RV	Right Ventricle
SA	Sinoatrial
SEM	Standard Error of the Mean
SL	Semilunar Valve
SV	Stroke Volume
TPG	Transvalvular Pressure Gradient
VSD	Ventricular Septal Defect

# 1. Literature Review

## 1.1. The Anatomy of Heart

The heart is a very efficient blood pump, pumping the blood to the whole body via the circulatory system. Blood circulation in the body is essential since the blood carries oxygen, nutrients and supplies it to all tissues in the body as well as removing carbon dioxide and waste products out of the tissues. The heart is located centrally in the thoracic cage, between the right and left lung sitting on the diaphragm as it is shown in Figure 1a. The size of the heart varies depending on the gender, age, size and the condition of the heart. <sup>2</sup>

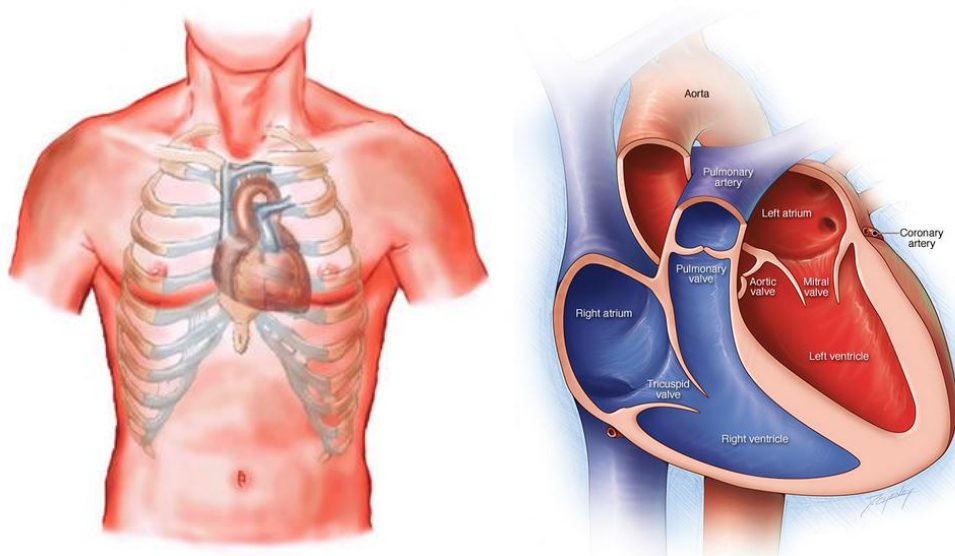


Figure 1: (a) Location of the heart in the body. <sup>3</sup> (b) Anatomy of the heart. <sup>4</sup>

In the heart, there are three layers within the heart muscle. The innermost layer, endocardium, is a thin, bright layer, which lines the chambers inside the heart. The myocardium is the middle layer which is composed of striated muscle tissue with a non-uniform thickness along the heart and causes the contraction. Lastly, the epicardium is a thin outer layer made of elastic ligaments on the surface of the heart. The heart is placed in the pericardium which is a connective tissue layer around the heart. It protects and stabilizes the heart and associated vessels in the mediastinum, as well as lubricates it. It also protects the heart from infections and prevents from excessive dilatation. <sup>2</sup>

The heart is divided into two halves, right and left, by a wall of muscles called the septum as shown in Figure 1b. Each half has an atrium and a ventricle, resulting in four chambers: the right atrium, right ventricle, left atrium and left ventricle. All heart chambers carry an equal volume of blood, but the left ventricle owns the thickest chamber wall. The right side of the heart pumps deoxygenated blood to the lungs, meanwhile the left side of the heart pumps oxygenated blood to the systemic system of the body.

Inside the heart there are four heart valves that direct a one way flow of blood, also shown in Figure 1b. They can be divided into two main types – atrioventricular valves (AV) and semilunar valves (SL). Atrioventricular valves can be found between the atrium and ventricle, particularly the tricuspid valve located on the right side of the heart and the mitral valve located on the left side of the heart. Another two valves, the aortic valve located between the left ventricle and the aorta and the pulmonary valve between the right ventricle and the pulmonary artery, are called semilunar valves because their leaflets have the shape of a half moon.<sup>2,5,6</sup>

The main difference between both types of valves lies in the atrioventricular valve leaflets being attached to the ventricular wall by papillary muscles and chordae tendinae in order to prevent leaflet prolapse back into the atrium during systole.<sup>7</sup> Both types of valves are considered to have a passive function. Although with further research, atrioventricular valves are now being reconsidered as active structures since there is evidence of motory and sensory innervation, particularly in the mitral valve. To support the evidence, contractile cells have been proved to be found in mitral valves, and it is believed that nerves and cells together are participating in valve movement and tone. Semilunar valve leaflets have no active opening, and rely on the relative pressure changes over a period of a cardiac cycle.<sup>7,8</sup>

## **1.2. Blood Circulation**

The blood circulation is performed in the body on two main levels. Firstly, the pulmonary circuit which relates to the lungs, takes deoxygenated blood from the right ventricle (RV) through the pulmonary valve and pulmonary artery directly to

the lungs, where the blood gets oxygenated and then goes through the pulmonary vein to the left atrium (LA), passes the mitral valve (MV) to the left ventricle (LV). Secondly, the systemic circuit involves the rest of the body and originates from the left ventricle (LV) carrying oxygenated blood with nutrients and hormones through the aortic valve directly to the aorta which supplies upper and lower part of the body due to its branching. The blood is carried in the arteries towards the organs and tissues, and then takes deoxygenated blood with carbon dioxide and waste products via venous circulation, through the superior and inferior vena cava back to the heart where blood enters the right atrium (RA). Blood then passes through the tricuspid valve directly to the right ventricle (RV). The whole circulatory system of blood in the body is shown in Figure 2. <sup>2,6</sup>

The frequency of the cardiac cycle is the heart rate, and is calculated as the number of contractions of the heart in one minute. It is always expressed as “beats per minute” (bpm). When the heart is at rest, presuming a heartbeat of 70 bpm, it beats 100,000 times a day and about 35 million times a year. <sup>2,6</sup>

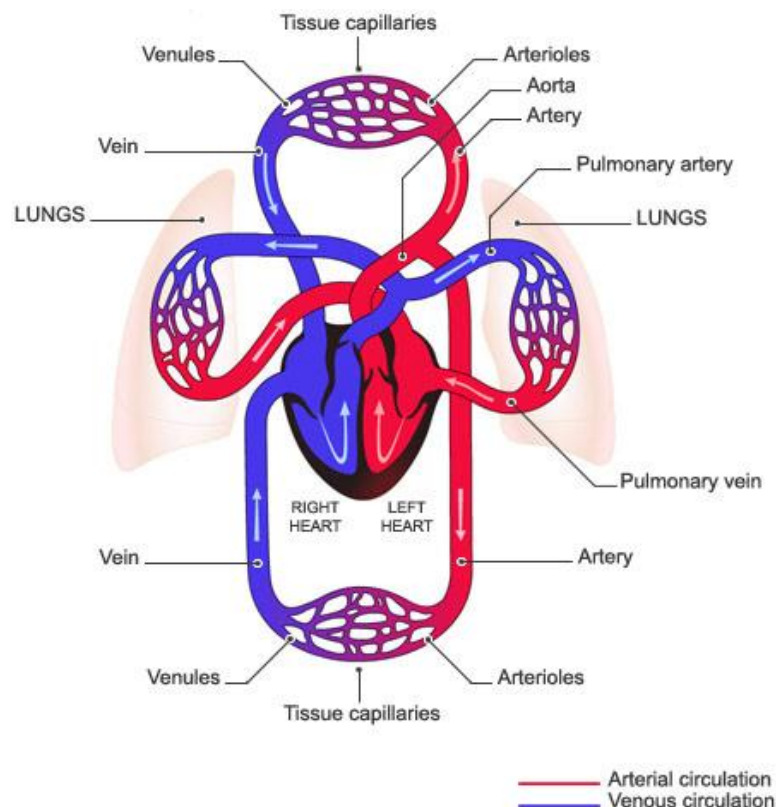


Figure 2: Circulatory system of blood in the body. <sup>9</sup>

The heart needs a blood supply to itself as well. Since the heart owns many layers, nutrients cannot diffuse from the chambers through the entire heart, therefore the coronary circulation is responsible for a blood supply to the myocardium. Both right and left coronary arteries originate from the aortic valve sinuses and deliver blood to the myocardium and other components of the heart. <sup>2,6</sup>

### 1.3. Cardiac Cycle

The whole cardiac cycle starts with complete cardiac relaxation, the atrioventricular (AV) valves are open, this happens only during the atrial and ventricular diastole. Blood returning from the body and lungs fills the atrium, and then freely flows to the ventricle through the open AV valves. Once the ventricles are three-quarters full, the SA node sends the impulse to the atria which causes atrial systole and the rest of the blood is ejected to the ventricle. The electrical impulse is propagated towards the AV node, where after some delay it spreads to the ventricles. Once atrial systole is completed, it allows the ventricles to contract, which causes ventricular systole. At the same time, the atrium gets to the diastolic phase, which stays until the next cardiac cycle. In order to close the AV valves, pressure in the ventricles has to exceed the atria one. This also happens during the ventricular systole. With AV valves closing, increasing pressure in the aorta and the pulmonary artery opens the SL valves to send the blood into the great arteries and then into the whole body system. After ventricular systole is completed, ventricular diastole begins. Since the pressure in the arteries is decreasing, SL valves close so the blood cannot enter the ventricles again. Blood is then ejected to the lungs and rest of the body – pulmonary artery and aorta. At this point, the cycle starts again with relaxation both the atria and ventricles and AV valves open. <sup>2</sup>

There are two main heart sounds one can observe. The first heart sound is a low prolonged sound “lubb” caused by closure of both mitral and the tricuspid valves at the beginning of ventricular systole with a duration of 0.15 seconds and a frequency of 25-45 Hz. The second sound is rather shorter and has a higher sound “dub” caused by closure of the aortic and pulmonary valves just after the end of ventricular systole with a duration of 0.12 seconds and a frequency of 50 Hz.

Between the second sound and the next cardiac cycle, there is a pause, which takes around 0.8 seconds.<sup>10</sup>

## **1.4. The Heart Valves**

### **1.4.1. Anatomy of the Heart Valve**

The heart valve is considered a highly organized structure of connective tissue with dynamic cell populations. In embryos, valvulogenesis occurs right after the early stages of cardiogenesis and creates endocardial cushioning and remodelling of the extracellular matrix (ECM). Therefore valvular anatomy is very complex. Despite the fact, that all valves have common functional requirements, each of the heart valves have specific intrinsic structures, and therefore the individual cusps and leaflets can observe distinct characteristics, that can determine its vulnerability to diseases.<sup>10,11</sup>

As mentioned before, there are four valves divided into two main types of valves observed in the heart, the tricuspid and mitral valves are atrioventricular (AV) valves which separate the atria from the ventricles. Meanwhile the aortic and pulmonary valves are semilunar (SL) valves, separating the ventricles from the great arteries (aorta and pulmonary artery). The shape of the annulus depends on the type of valve, AV valves are large asymmetric leaflets forming a ring-shaped annulus however, SL valves have a crown-shaped annulus represented by an aortic valve, resulting in the shape of individual cusps. The AV valve is attached to the ventricular wall by highly elaborated system consisting of papillary muscles and chordae tendinae. Important support to the heart valves, especially tricuspid, mitral and aortic valve is provided by the annulus fibrosa made up of interconnected, fibrous and cartilage-like apparatus.<sup>10,11</sup>

Looking at a particular heart valve, the aortic valve consists of three cusps named after the relations to the coronary arteries – the noncoronary, right coronary and left coronary cusps. However, the pulmonary valve is located leftward to the aortic valve, and its cusps are aligned in an orthogonal plane. The mitral valve consists of two leaflets – anterior and posterior. The mitral valve also has a highly elaborated system consisting of papillary muscles and chordae tendinae preventing the leaflets prolapsing back to the atrium. The anterior leaflet is in continuity with the aortic

valve, unlike the pulmonary valve which is separated by a muscle wall from the tricuspid valve. <sup>10,11</sup>

The thickness of the human valve varies across the entire tissue, but is typically less than 1 mm. Valves on the left side of the heart are slightly thicker than valves at the right side of the heart as well as AV valves display higher thickness than the SL valves. <sup>10,11</sup>

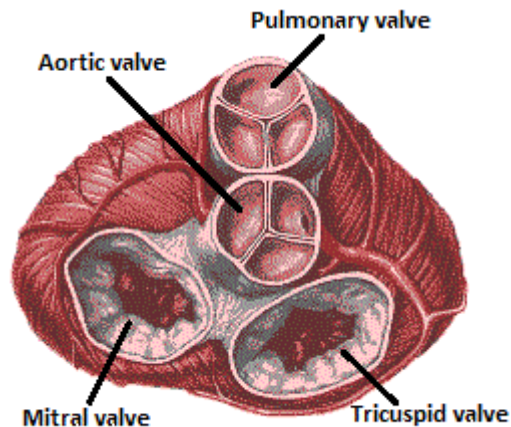


Figure 3: Distribution of valves in the heart. <sup>12</sup>

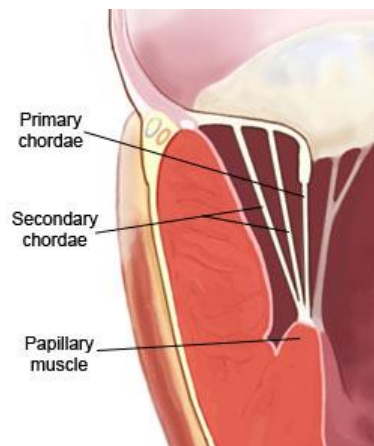


Figure 4: Papillary muscles and chordae tendinae. <sup>13</sup>

#### 1.4.2. Fluid Dynamics of the Valves

The heart valve is not a static structure, even in its natural state, there is always some motion of the leaflets. The motion causes the valve to open and close, and is the most significant feature of the heart valves. Capturing the valve moment is only possible using special techniques, especially high-speed recording due to the valve's rapid movement around 17 to 20 ms. <sup>14</sup> Several different techniques are used such as fluoroscopy (use of markers) and aortic root cineangiography (use of X-ray), in



case of in vitro study a pulse duplicator system was used in which a clear liquid is pumped through the valve.<sup>5,14,15</sup>

The heart valves in general have a very important function to allow blood flow in only one direction without causing any significant resistance to blood flow which would put an extra demand on the heart itself. It also has to function with almost 100% efficiency as well as not use much energy to open and close the valve. All these considerations have to be taken into account when looking at the dynamics of the valve.<sup>5,14,15</sup>

Coming back to the leaflets motion, one would say there is no movement taking place when the valve is either open or closed, but while the valve is open, the leaflets gradually move towards the valve centre, resulting in a gradual decrease in distance of the valve leaflets. During the early stages of systole, the valve is maximally open, and then gradually closes during process of systole, and at the end of the systole it rapidly closes with minimal regurgitation. The orifice of the valve happens to be circular (or nearly). As the leaflets move toward the valve centre, the orifice gradually changes during systole and can be observed from being circular towards triangular depending on which angle it was taken from. There are also several factors influencing the orifice such as condition of the myocardium, dynamics of the aortic root, and the cardiac output.<sup>5,14,15</sup>

The blood flow through the valves is mainly laminar and flat with a peak velocity of approximately  $1.35 \pm 0.35$  m/s in the first third of the cycle. During systole, the commissure radius, a distinct area where all leaflets come together and create an annulus, expands by 12%, and decreases during the diastole by 16%. Valve leaflets also contract circumferentially during systole in order to increase the orifice area as well as radially extend during diastole to ensure the valve fully coaptates.<sup>15</sup>

### **1.5. Congenital Heart Diseases**

Congenital heart disease is one of the most common defects present at birth, affecting up to 9 babies in every 1,000 born in the UK.<sup>1</sup> As the word congenital explains a condition present at birth, this type of heart disease affects one of the most vulnerable groups in this society, the babies. If not treated right from the

beginning, it can develop into significantly more serious disease affecting their future life. Symptoms of paediatric congenital heart disease are often discovered during the routine physical examinations which could be: troubles with breathing, bluish tones to the skin (cyanosis), poor eating habits, rapid heartbeat and tiredness (fatigue). Congenital heart diseases seriously affect the blood flow in the body, resulting in mixing the oxygenated and deoxygenated blood together causing problems to organs and tissues as they're not receiving the right amount of oxygenated blood.<sup>6,16</sup>

There are various types of congenital heart defects that develop before the birth, affecting the blood flow through the heart after the birth. The first of the diseases to be mentioned are Septal Defects. A septal defect can be described as a hole in the septum which divides the heart. Having a hole in the wall causes mixing of the blood from both sides of the heart. They can be divided into two main groups: Atrial Septal Defects and Ventricular Septal Defects. Atrial Septal Defects (ASD) are holes between a wall which separates the left and right atria, preventing the blood to flow into the left ventricle as it should. Ventricular Septal Defects (VSD) are holes between a wall which separates the left and the right ventricle, resulting in allowing the blood to flow from the left ventricle to the right ventricle instead of flowing into the aorta and into the whole body as it should. VSDs represent approximately 20% of all congenital heart diseases and require surgical corrections.<sup>6</sup> The holes are of various sizes, the bigger the holes, the bigger the complications it causes.<sup>6,16</sup>

Congenital heart diseases also involve heart valves. There are various types of heart valve defects. The first of them is stenosis (narrowing) that occurs if the valve's cusps thicken, get stiffer or even fuse together. In this case the valve is not able to fully open and it puts a higher demand on the heart as it has to work harder in order to pump blood through the valve. Such an example could be a Bicuspid Aortic Valve which is the most common type of congenital aortic valve disease, affecting approximately 1 in 50 people.<sup>17</sup> Bicuspid Aortic Valve occurs when the aortic valve has instead of three cusps only two which can be seen in Figure 5.<sup>6,16</sup>

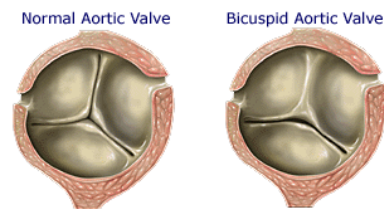


Figure 5: Normal Aortic Valve on the left side, Bicuspid Aortic Valve on the right side. <sup>18</sup>

Another heart valve defect observed is Atresia which causes a missing opening in the heart valve for blood to pass through. This defect is considered as more complex congenital heart disease. The last heart valve defect is Regurgitation. This defect causes the valve to not close properly, allowing the blood to leak back through the valve. The most common heart valve defect is Pulmonary Valve Stenosis resulting in a narrowing of the heart valve, putting a higher demand on the heart. <sup>6,16</sup>

Coarctation of the Aorta is another defect, defined as a narrowing of the descending aorta. It causes the left ventricle to work harder in order to push the blood through the narrowed aorta. The degree of the obstruction of the Aorta can vary, therefore there is a classification system of narrowing of the aorta for easier diagnosis. <sup>6</sup>

In the world, there are many more congenital heart diseases than the ones mentioned above. As congenital heart defects are more complex, there can be more than one defect present at the same time.

### 1.6. Treatment strategies for Paediatrics

Treatment of paediatrics brings totally different perspective to the health care strategies. The scale the treatment is performed on is much smaller taking into account that the paediatric heart is five times smaller than adult heart. <sup>6</sup> And this represents a challenge for current medical care. The small body is subjected to many changes over time. The baby is growing and all organs and tissues with him/her as well. Therefore current medical care has to face a big challenge in a constantly changing environment, especially the growing heart as well as the heart valves. The goal of the treatment strategies is to develop potentially deliverable long-term outcome that would make the treatment easier.

When reconstruction fails, replacement becomes the only option. Current strategies use homograft and bioprosthetic valves in order to obtain the same haemodynamic profile with regular heart valves. On the other hand use of mechanical prostheses is limited due to the risk of thromboembolism.

The first of the treatment strategy is the Melody Valve which is performed with a transcatheter pulmonary therapy that is widely used not just for paediatrics but also for adult patients. This therapy does not require an open heart surgery which brought a big contribution to the medical care. The bioprosthetic heart valve consists of a bovine jugular vein valve sutured within a platinum iridium frame as it is shown in Figure 6.<sup>19</sup>



Figure 6: Melody valve.<sup>20</sup>

The procedure is performed with the bioprosthetic valve crimped onto the catheter which is inserted into the vessel in the patient's groin. The catheter is guided through the vessel to the heart with a help of an echocardiography or fluoroscopy where the old valve is replaced by the new one by inflating the balloon which expands the bioprosthetic heart valve enabling to take over the valve function. Having an inflatable balloon allows to expand the bioprosthetic valve as much as the surgeon needs which helps the heart valve replacement in paediatrics.<sup>19</sup> The replacement of the heart valve is performed a few times over the lifespan due to the short durability of the bioprosthetic heart valve. At the Children's Hospital in Boston, USA, they have successfully implanted a modified version of an expandable prosthetic heart valve in several children with mitral valve disease. They used a Transcatheter therapy in order to implant the expandable bioprosthetic heart valve to be able to enlarge the bioprosthesis as the child grows. The expansion of the

bioprosthesis could be done with a catheter containing an inflatable balloon as the heart of the child grows.<sup>21</sup>

Another treatment strategy is the Ross procedure which has been named after the cardiac surgeon Donald Ross in 1962 who proposed this technique first. This procedure is most commonly used for the aortic valve replacement (AVR) and uses the pulmonary autograft of the patient in the aortic position which has brought a great advantage in treatment strategies for paediatrics. The pulmonary heart valve is then replaced by an allograft from human cadavers. The Ross procedure has a long-term durability, an excellent haemodynamic profile of the pulmonary autograft, and no need of anticoagulation to prevent thromboembolism. On the top of that, there is a potential with the Ross procedure for further growth of the autograft.<sup>22,23</sup>

When a bioprosthetic valve is developed to be deployed in a human, testing of such a valve has to be performed prior to the deployment in a testing device designed for the heart valves, the valve tester. There are different types of valve testers such as durability heart valve tester or pulse duplicator. In order to prove the durability of the heart valve, 200 million cycles have to be tested on the bioprosthetic valve. In this project, the pulse duplicator has been chosen to undertake the testing of the bioprosthetic aortic heart valve. The pulse duplicator has two chambers, left ventricular chamber and the aortic chamber. In these two chambers, a bioprosthetic heart valve is placed which simulates the natural environment of the aortic valve. This testing device provides information about the pressure distribution across the heart valve known as the transvalvular pressure gradient (TPG), flow velocity through the valve, effective orifice area (EOA) and others.

## 2. Aims and Objectives

The aim of this thesis is to develop an expandable testing apparatus for growth compensating paediatric heart valves which could be employed in the future to deliver high medical excellence for very young patients.

Objectives of this thesis can be specified as:

- Establishing the design of an expandable test holder that could be used in the valve testing environment of the pulse duplicator.
- Performing set of tests in pulse duplicator tester to collect and analyse data of the bioprosthetic heart valve held in the expandable holder.
- Future solutions with an automated holder for the growth compensating paediatric heart valve.

Having a design that would perfectly fit into the testing requirements of growth compensating paediatric heart valves is the key part of the project. Therefore a sufficient amount of time has to be spent in choosing the right design for the valve holder. Once the right design is chosen, it was 3D printed. While waiting for the model to be printed out, setting up the pulse duplicator for heart valve testing is another key part of the project. In order to obtain the data to perform the proper analysis, a set of tests has to be carried out. To study the relationship between the valve annulus and increasing frequency, first set of experiments with no valve held in place was performed. Starting from that, it can be further predicted how the haemodynamic profile of the bioprosthetic heart valve will look like in relation to expanding/crimping annulus as well as increasing frequency of the fluid flowing through the valve. Eventually, testing with a valve held in place is performed in order to assess the haemodynamic properties of bioprosthetic heart valve. Once the testing is done and data are successfully collected, analysis of the data can be performed. And from that the pressure distribution across the bioprosthetic heart valve can be presented and discussed.

On the top of that, in order to improve the entire testing apparatus, an automated system is considered as a future perspective that could be deployed in further research and testing. A quick overview on how this issue could be developed is explained in the Chapter 6 on the future perspectives.

## 3. Methodology

### 3.1. Introduction

This chapter presents design requirements and specifications required to develop an expandable valve testing apparatus as well as the undertaken experimental part of this project. The first and one of the most important parts of this project was to develop a design idea that could be further implemented in testing the heart valve. The basic parameter that has to be met is the expandable property of the testing apparatus. Starting from that, research has to be made to find available mechanisms on the market that would fit into the requirements and fulfil the desired function. The design has to be able to expand as well as crimp the valve in order to change the valve annulus to bring the current treatment strategies of heart defects closer to the natural environment.

### 3.2. Design

#### 3.2.1. Design Specifications

The design of the testing apparatus for the growth compensating heart valve is a complex issue that has to be dealt with on various levels. The mechanism has to be designed in a way to simulate the growth of a new-born, therefore starting from tiny dimensions less than 12 mm up to adult ones ranging 18 – 23 mm as the individual grows.<sup>24,25</sup>

In order to be able to design an expandable valve holder, desirable design requirements have to be met. Based on literature review, the following requirements were taken into account:

- **Minimal scale** – tiny dimensions present a big challenge in current treatment strategies due to the minimal scale that the treatment has to be performed on.
- **Expandable annulus** – ability to expand and crimp the annulus of the heart valve is an essential requirement for the valve holder.
- **Water resistance** – leaking of water introduces a different pressure distribution through the bioprosthetic heart valve which results in invalid



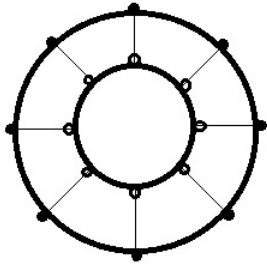
data readings while testing. Therefore the expandable mechanism has to be designed in way to prevent water leakage.



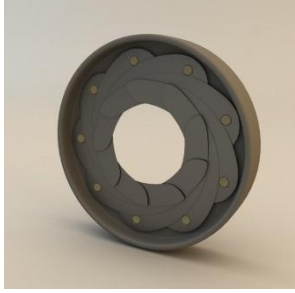
- **Valve attachment** - the entire mechanism has to ensure that the valve is not going to migrate during the testing. The bioprosthetic heart valve has to be held in place tightly, sitting in the holder without possible migration during the actual testing.
- **To fit into the testing device** – the expandable valve holder has to fit firmly in the testing device to be able to perform the testing.
- **Material** – rubber-like materials are desirable for use in 3D printing of expandable mechanisms due to its sealing, non-slipping, durable and flexible properties.<sup>26</sup> In case of bioprosthetic valve, material should be also bio-compatible.
- **Not damaging the valve** – the valve holder has to be designed in way to not damage the valve while crimping or expanding. If the bioprosthetic valve with a stent is used, the valve holder should not damage its skirt.
- **Automated mechanism** – the heart valve is desirably expanded or crimped by the mechanism itself without any manual help. This requirement will be discussed in Chapter 6 on the future perspectives.
- **Easy to manufacture** – 3D printing is a manufacturing option due to its ease in printing complex parts.

### 3.2.2. Design Ideas

Initially there have been three main ideas for designing the testing apparatus from which it was possible to choose. All design ideas are listed in Table 1.

Table 1: Design ideas.

Design	Description	Picture	Advantages	Disadvantages
1	A rubber elastic ring attached to the bigger tighter ring by strings. The annulus of the rubber ring could be		Elastic way of expandable annulus.	Strings would enable the valve moving freely in the tester. The water would leak through the holder,

	manually expanded with a help of strings attached.			therefore it is not stable to use. In this mechanism the heart valve would easily slip through it.
2	A hose clip. <sup>27</sup>		Controlled rate of expandable annulus. A rigid structure – valve would not migrate.	Attachment of valve to this apparatus is challenging.
3	A dumpling maker (kitchen equipment), engineering unrelated design idea based on expandable mechanism.		Uniform way of expanding the annulus.	Software modelling is challenging due to leaflets overlapping each other.
4	Iris mechanism. <sup>28</sup>		Uniform way of expanding the annulus. Can be automated. Different types of blades.	Crimping and expanding the valve can be challenging.

### 3.2.3. Design Concept

All the design ideas from the previous subchapter were reviewed and assessed. Taking into consideration design requirements, especially particular advantages and disadvantages brought together a final decision. The last design idea was chosen as a way to go due to its uniform way of crimping and expanding the annulus, holding the valve firmly preventing it from migration. Overlapped blades can also deliver prevention from water leakage through the mechanism. The system can be also automated.

In Figure 7 is shown the final outcome of 3D printing the expandable heart valve holder that was used for testing in this project. The material used was acrylonitrile butadiene styrene (ABS) plastic.



Figure 7: Iris mechanism idea, 3D printed parts.

### 3.3. Experimentation

This part of the chapter presents experiments undertaken in the frame of this project. Firstly, the device used for testing is presented. Then the experiments are further divided into three main parts:

- 1) Tests performed with the valve not in place.
- 2) Tests performed with the CoreValve.
- 3) Tests performed with the Iris mechanism without/with the CoreValve.

Figure 8 presents the entire testing device on which the testing was performed.



Figure 8: Testing device.

### 3.3.1. Pulse Duplicator

The pulse duplicator is a testing device consisting of two hydraulic components. The first component is pumping the solution into the circuit and the second component is simulating left ventricular chamber and aortic chamber. Between those chambers sits the heart valve holder where the bioprosthetic valve can be placed. In Figure 9 is shown the pumping system, and in Figure 10 is shown the testing system.

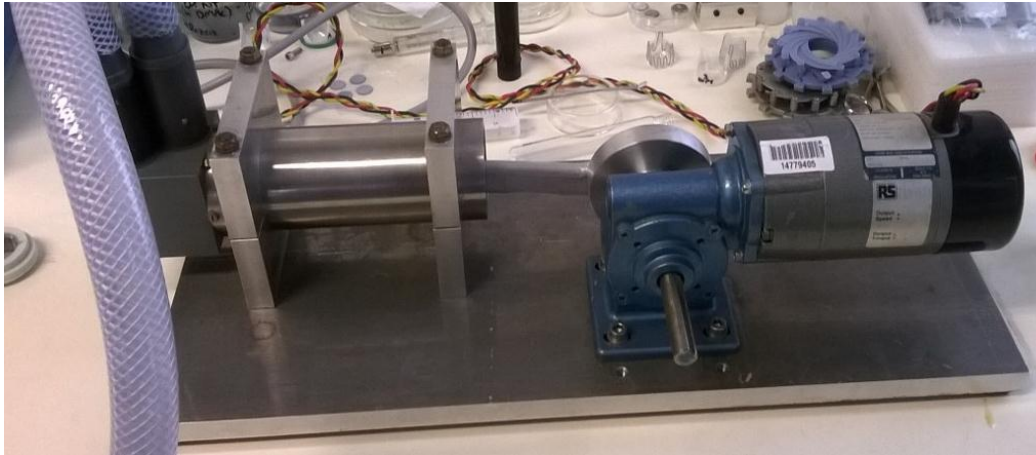


Figure 9: Pulse duplicator – pumping system.

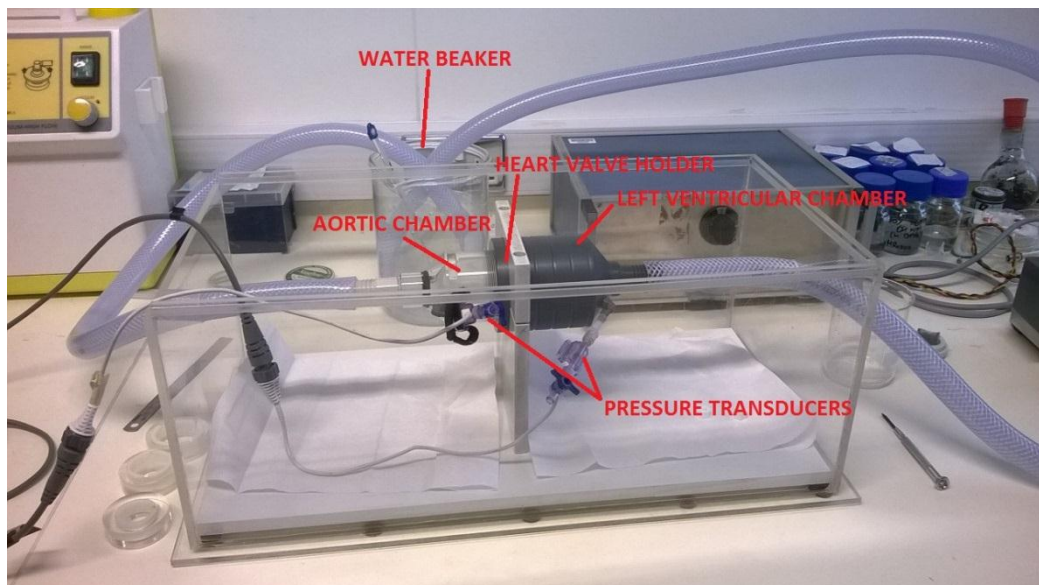


Figure 10: Pulse duplicator – testing system.

#### Pumping system

In this testing device shown in Figure 9, the solution is pumped from a container by a piston pump driven by an electric motor (Parvalux, Wallisdown, Bournemouth,

UK) with the speed up to 4000 rpm. The speed can be adjusted from speeds 1 to 11 representing increasing frequency of the pump (heart rate – 30 – 115 bpm, represented in Table 2). The solution is led through tubing up to the testing system. During systole, the solution is sucked from the reservoir (the water beaker) to the pump and forced through tubing up to the testing system and during diastole, the solution gets back to the reservoir.

### **Testing system**

This device simulates the left ventricle, aortic valve and the aorta as it is shown in Figure 10. The solution is pumped through the chambers, forcing the valve to open during the systole and close during diastole. In order to be able to measure the pressure gradient between those chamber, pressure transducers were placed onto the particular chambers, measuring the solution displacement. The pressure transducers are shown in Figure 10. The system of pressure readings belongs to a data acquisition system (BIOPAC, California, USA) and data were obtained through the software AcqKnowledge 4.1 (BIOPAC, California, USA).

As a testing medium, 22% glycerol/water solution was used to simulate the viscous properties of the whole blood.<sup>29</sup> For the whole circuit of the pulse duplicator, 2 litres of water and 440 ml of glycerol were put in.

While testing in the pulse duplicator, a few parameters have been possible to measure in order to simulate the natural environment, heart rate (HR), stroke volume (SV) and cardiac output (CO). HR is the frequency of the heart and is measured in beats per minute (bpm), in the testing apparatus it represents the frequency of the pump. SV is the amount of blood ejected by the left ventricular chamber during one contraction in the natural environment, here SV represents the amount of solution ejected by the pump and is measured in millilitres (ml). Final CO gives the volume of blood pumped per minute by each ventricle of the heart and is defined by Equation 1:<sup>6</sup>

$$CO(ml/min) = HR \times SV \quad (1)$$

All parameters are shown in Table 2.

Table 2: Parameters obtained from testing apparatus.

Speed	Heart Rate (HR) (bpm)	Stroke Volume (SV) (ml)	Cardiac Output (CO) (ml/min)
1	30	5	150
2	40	6	240
3	50	7	350
4	60	8	480
5	70	10	700
6	82	15	1230
7	94	30	2820
8	104	35	3640
9	115	40	4600

### 3.3.2. Valve Attachment

In this project, a bioprosthetic heart valve made of porcine pericardium with self-expanding Nitinol frame known as the CoreValve (Medtronic, Minneapolis, USA) was used, with a diameter of 29 mm, an upper diameter 38 mm and a bottom diameter 24 mm and is shown in Figure 11.

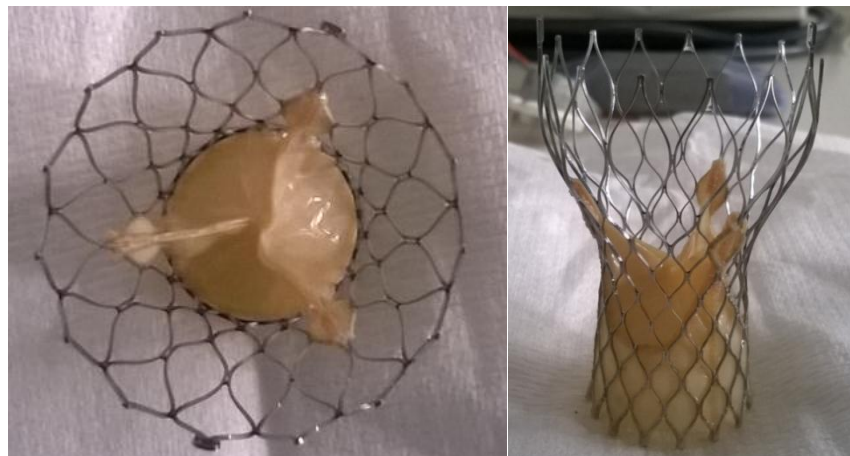


Figure 11: CoreValve, heart valve used for testing: (a) top view. (b) front view.

Regarding how the valve was held in place, literature research was performed in order to find the best way of placing the valve onto the holder. Due to its minimal dimensions, the choice was quite limited. Using small hooks that would fix the valve in place, or implementing small magnets turned up to be not feasible due to the

small size of the holder. This valve owns a stent which brought another insight in finding a way to not damage the stent while placing the valve onto the valve holder. Therefore hooks and other rigid tools were eliminated as they could seriously damage the bioprosthetic heart valve. The best way to place the valve in the holder was through using silicone moulding material. A silicone mould was manually prepared to deliver the best attaching properties for the bioprosthetic heart valve. For this purpose, a slow setting type of silicone mould was used. For moulding the silicone rings, 25, 27, 31 and 33 mm testing rings were used. An example of the silicone placed in the holder as well as the valve placed onto the holder is shown in Figure 12.



**Figure 12: Valve attachment: (a) a holder with silicon mould, (b) the heart valve placed onto the holder.**

The challenge the silicon moulded attachment represents is if done manually, the annulus will not have the accurate shape as if the silicon ring would be manufactured by a machine.

In case of testing the CoreValve in Iris mechanism, a thin film called parafilm (Bemis, Wisconsin, USA) was placed on the valve in order to protect the valve's skirt from damaging when putting it into the Iris mechanism. Because the blades are overlapping and are not into one uniform layer, it could cause a serious damage to the CoreValve skirt, creating the holes in the skirt and disturbing the bovine pericardium which would result in not being able to test with this valve anymore.

### **3.3.3. Testing**

Testing was performed in 3 main stages:

### **3.3.3.1. Valve not in place**

The first set of experiments has been performed with the valve not held in place. These tests have been performed to gain a better understanding of the testing device as well as studying the relationship between the annulus size and increasing frequency to further be able to predict the testing with the valve held in place. The collected data can also be considered as a base line data for further testing.

The experiments were run on different frequencies (considered the heart rate) ranging from 30 bmp up to 115 bpm as well as four different diameters: 33 mm, 31 mm, 27 mm, 25 mm. The experiments were run on each of the diameters separately, all frequencies have been tried on. The important part of the experiments was to ensure the transducers were in line with the pressure ports to not cause high pressure readings. This rule applied to all the experiments. Before each part of the experiment a trial pressure reading was performed to ensure the accuracy of the readings. The pressure readings have been obtained from two channels, the first placed on the left ventricular chamber, and the second placed on the aortic chamber. Both channels were used for determining the pressure drop measured across the heart valve known as the Transvalvular pressure gradient (TPG). The TPG is desirably as low as possible to not put an extra demand on the heart and it is obtained subtracting channel 1 (left ventricular chamber) from channel 2 (aortic chamber).

### **3.3.3.2. The CoreValve testing**

The second set of experiments was performed with the CoreValve held in place. These tests have been performed in order to test the best attachment of the valve as well as to test the CoreValve itself. Firstly, the CoreValve had to be washed in phosphate buffered saline (PBS) solution (Sigma-Aldrich, UK). The solution was obtained by dissolving a tablet in 200ml of distilled water. This solution was used for the rest of the experiments. At this point, a 22% glycerol/water solution was introduced into the circuit in order to better simulate the viscous properties of blood.



The experiments were again run on different frequencies ranging from 30 bmp up to 115 bmp with three different diameters: 23 mm, 20 mm, 16 mm. The valve annulus was crimped manually with attention to not damage the valve skirt as well as to fit into the diameters mentioned above. For better attachment of the valve, silicon moulded rings were used to provide sealing, ensuring the valve would not migrate during the testing. The experiments were run on each of the diameters separately, all frequencies have been tried on. The TPG was measured as before. Testing with CoreValve is shown in Figure 13 and 14.



Figure 13: CoreValve placed in Pulse Duplicator.



Figure 14: Valve attached to a holder: (a) side view, (b) bottom view.

### 3.3.3.3. Iris mechanism without/with the CoreValve

The third set of experiments was performed with the Iris mechanism with the CoreValve held/not held in place. These tests have been performed in order to test the expandable mechanism of the Iris with/without the CoreValve. The first three experiments were again run on different frequencies ranging from 30 bmp up to 115 bmp with three different diameters: 22 mm, 16 mm, 9 mm without the

CoreValve held in place. The fourth experiment was run as well on different frequencies ranging from 30 bpm up to 115 bpm with a fixed diameter of 22 mm and the CoreValve held in place. The valve annulus was again crimped manually with attention to not damage the valve skirt as well as to fit into the diameters mentioned above. At this point, parafilm, a thin elastic layer has been introduced to protect the CoreValve's skirt when putting onto the expandable mechanism. The experiments were run on each of the diameters separately, all frequencies have been tried on. The TPG was measured as before. Testing with the Iris mechanism is shown in Figure 15, 16 and 17.



Figure 15: Iris mechanism placed in Pulse Duplicator: (a) bottom view 22 mm annulus, (b) bottom view 16 mm annulus.



Figure 16: CoreValve placed onto Iris mechanism in Pulse Duplicator.



Figure 17: CoreValve placed onto Iris mechanism.

## 4. Results

This chapter brings together results from all parts of the experimental part of the project which were undertaken. Experiments were taken in three main stages. Firstly, with the heart valve not held in place in order to get familiar with the testing device. Secondly, experiments were run with the CoreValve attached to the tight valve holder with the silicone mould. And finally, experiments with Iris mechanism with or without the CoreValve were performed. All experiments were run with different diameters and speeds in order to study the relationship between the decreasing/increasing sizes of annulus as well as increasing frequency of pumping which simulates the heart rate. The next part of the Chapter 4 will be broken down into three main parts according to the undertaken experiments.

### 4.1. Valve not in place

This part of experimental work of the project has shown that the bigger the size of annulus is, the lower the pressure readings are. Taking it the other way around, as the diameters were smaller, the pressure of water going through the holder was higher. Therefore tests run with 33 mm diameter had considerable lower values of TPG than tests run with 27 mm or 25 mm diameter which was the smallest one. At lower frequencies, values of TPG were quite similar for the three biggest diameters (33 mm, 31 mm, 27 mm) however, the values have been twice or three times higher for the smallest diameter (25 mm).

Another observation is regarding the pump frequency. The higher the frequency is, the higher pressure readings are obtained. For two of the diameters (33 and 25 mm) a comparison of three frequencies (40, 70 and 104 bpm) is shown below to introduce the differences between the pressure readings expressed by TPG (Figures 18 – 23).

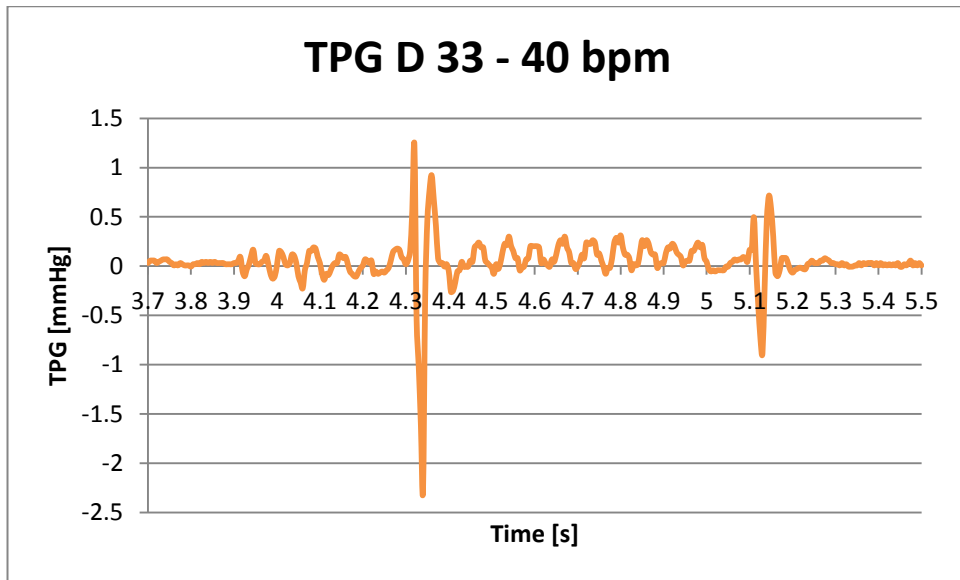


Figure 18: No valve in place – TPG of second cycle measured at 40 bmp, 33 mm diameter.

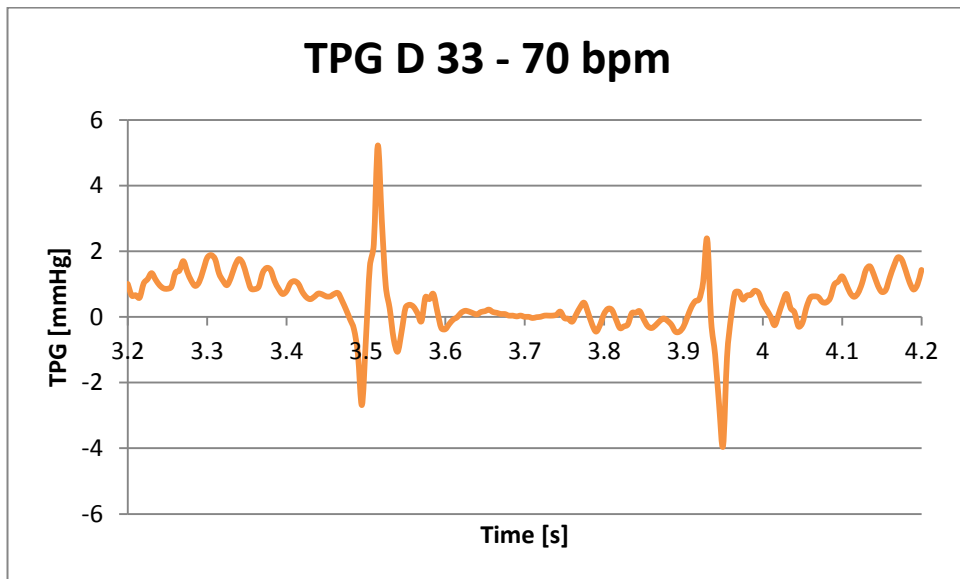


Figure 19: No valve in place – TPG of second cycle measured at 70 bmp, 33 mm diameter.

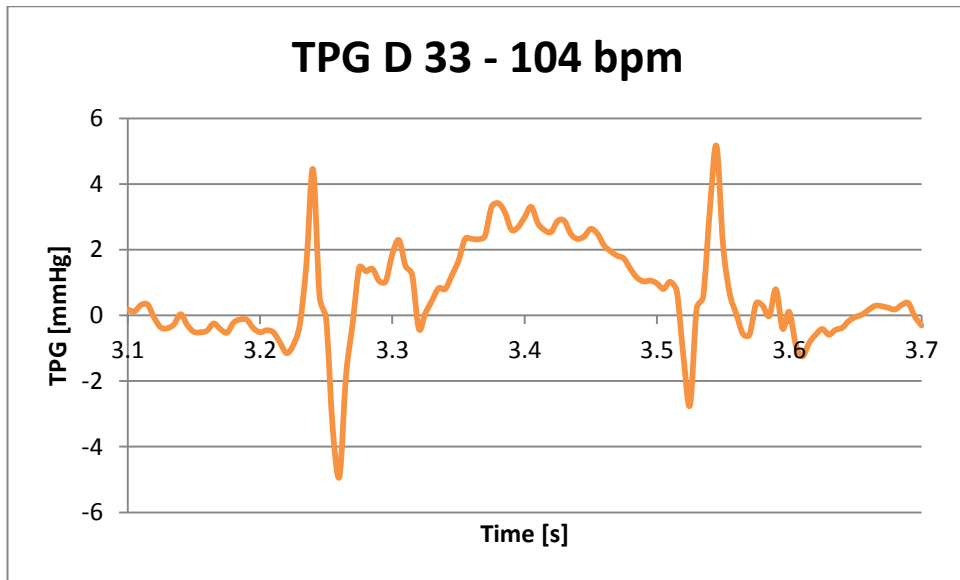


Figure 20: No valve in place – TPG of third cycle measured at 104 bmp, 33 mm diameter.

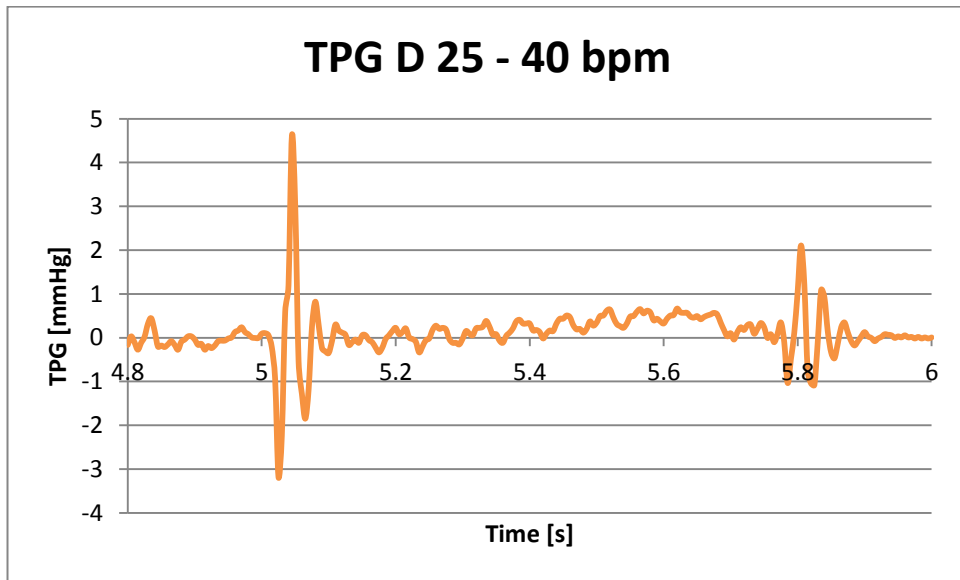


Figure 21: No valve in place – TPG of third cycle measured at 40 bmp, 25 mm diameter.

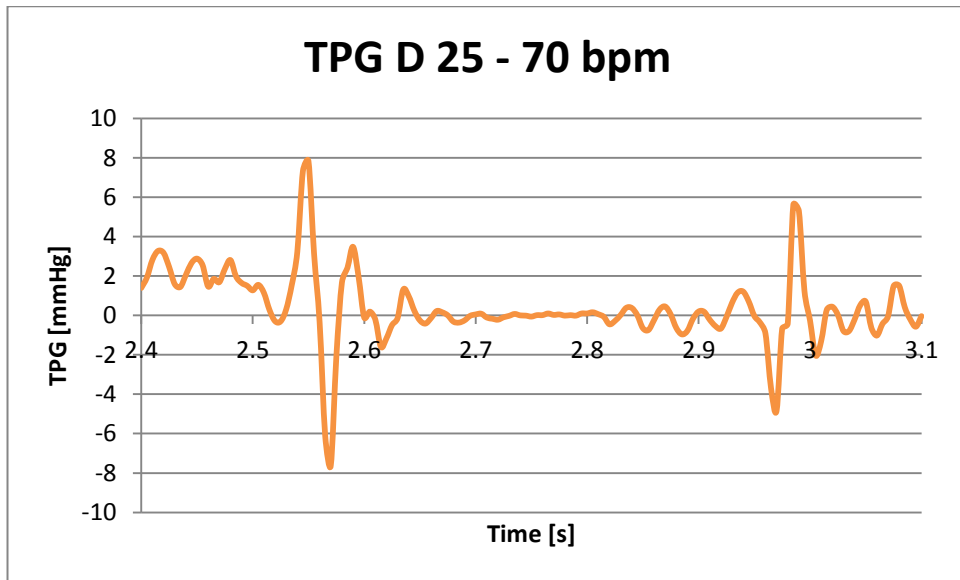


Figure 22: No valve in place – TPG of third cycle measured at 70 bpm, 25 mm diameter.

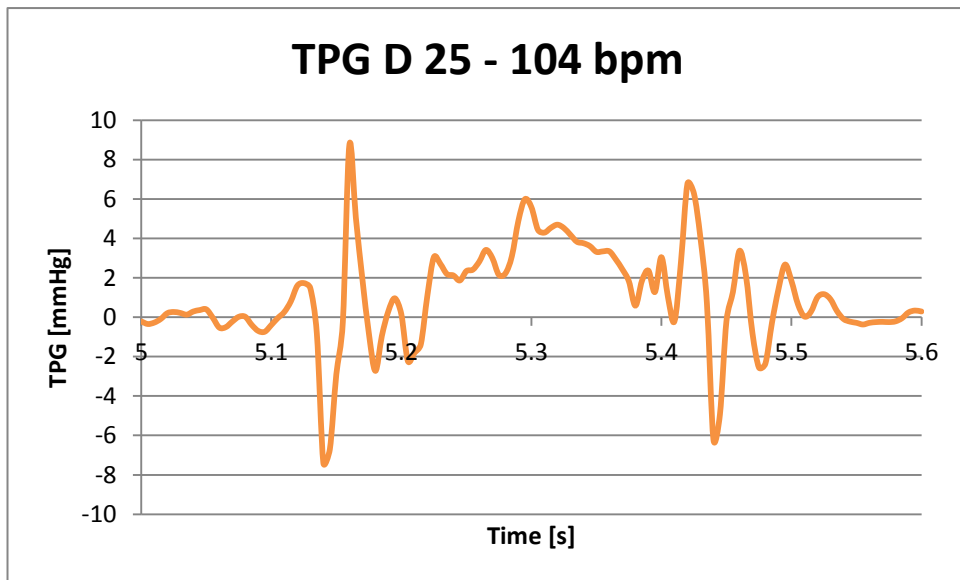


Figure 23: No valve in place – TPG of eighth cycle measured at 104 bpm, 25 mm diameter.

In Table 3 is shown the average  $\pm$  standard error of the mean (SEM) of 3 maximal values of TPG of each experiment in order to see the pressure changes when the annulus and frequency is increased. Figures 24 - 27 represent data taken from the Table 3 in bar charts with error bars. As it is seen in Figures 24 - 27, the relationship between frequency and annulus is not linear in each of the diameters. Linear behaviour can be observed at 31 and 27 mm diameters. The biggest 33 mm diameter and the smallest 25 mm diameter are not behaving uniformly, especially

starting from higher frequencies around 70 bpm, values tend to be similar with a decline at 104 bpm and then again a rise at the fastest 115 bpm.

Table 3: No valve in place - average  $\pm$  standard error of the mean (SEM) of 3 maximal values of TPG, 33, 31, 27 and 25 mm diameters.

	D 33	D 31	D 27	D 25
HR	AVG $\pm$ SEM	AVG $\pm$ SEM	AVG $\pm$ SEM	AVG $\pm$ SEM
(bpm)	(mmHg)	(mmHg)	(mmHg)	(mmHg)
30	1.02 $\pm$ 0.06	0.44 $\pm$ 0.01	1.24 $\pm$ 0.03	4.38 $\pm$ 0.09
40	1.22 $\pm$ 0.02	0.42 $\pm$ 0.02	1.47 $\pm$ 0.05	4.48 $\pm$ 0.24
50	1.38 $\pm$ 0.09	1.42 $\pm$ 0.23	2.03 $\pm$ 0.15	5.55 $\pm$ 0.32
60	1.86 $\pm$ 0.04	2.12 $\pm$ 0.1	2.22 $\pm$ 0.1	6.55 $\pm$ 0.13
70	4.67 $\pm$ 0.3	2.68 $\pm$ 0.03	3.5 $\pm$ 0.34	8.52 $\pm$ 0.1
82	5.37 $\pm$ 0.4	4.07 $\pm$ 0.12	5.2 $\pm$ 0.7	8.9 $\pm$ 0.14
94	5.49 $\pm$ 0.12	5.2 $\pm$ 0.46	7.04 $\pm$ 0.32	9.17 $\pm$ 0.44
104	4.41 $\pm$ 0.07	6.9 $\pm$ 0.33	8.7 $\pm$ 1.2	8.63 $\pm$ 0.1
115	4.93 $\pm$ 0.26	6.81 $\pm$ 0.17	10.25 $\pm$ 0.55	11.01 $\pm$ 1.22

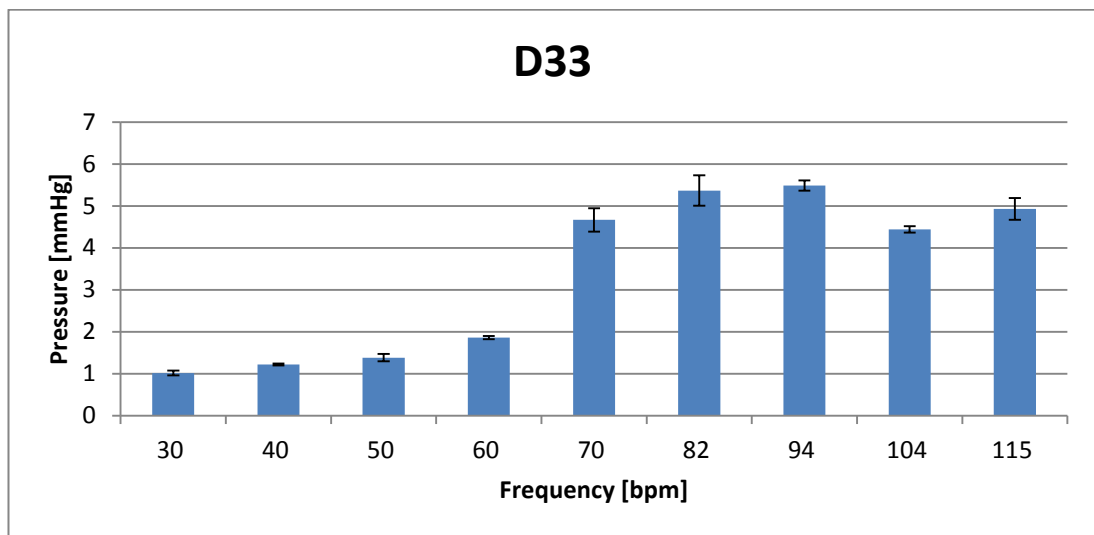


Figure 24: No valve in place - average TPG values represented for 33 mm diameter in bar chart with error bars.



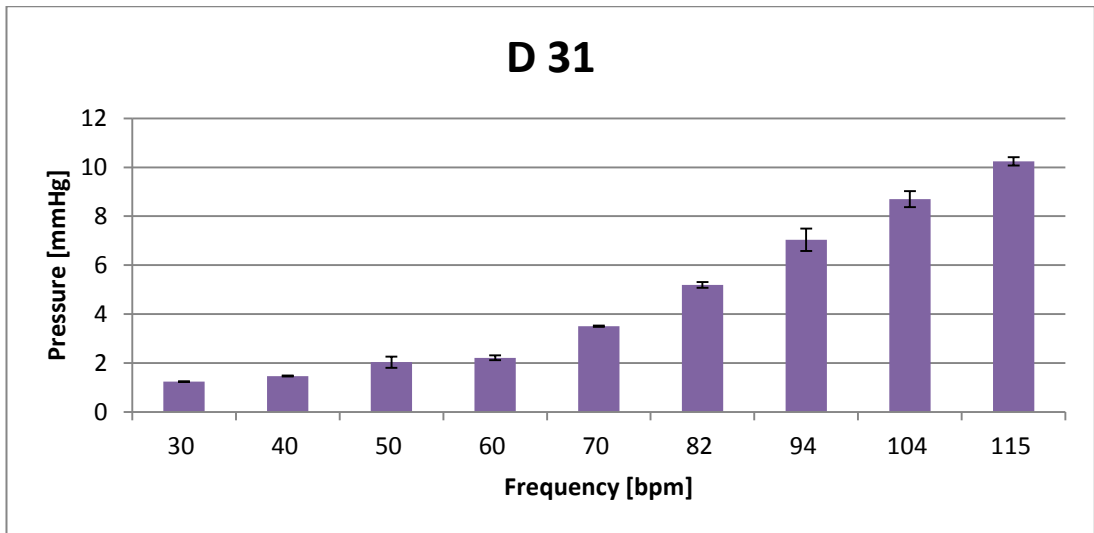


Figure 25: No valve in place - average TPG values represented for 31 mm diameter in bar chart with error bars.

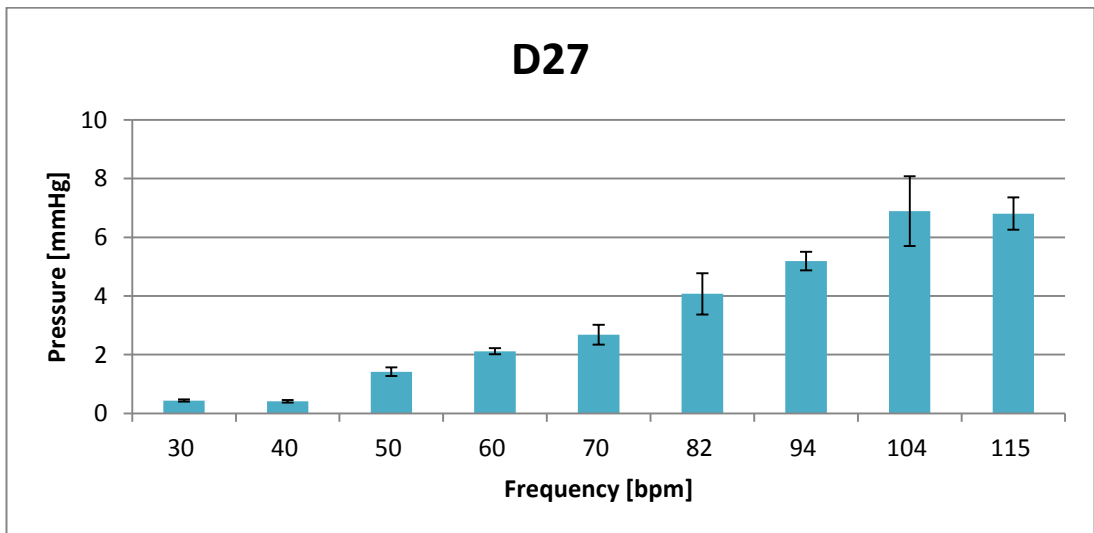


Figure 26: No valve in place - average TPG values represented for 27 mm diameter in bar chart with error bars.

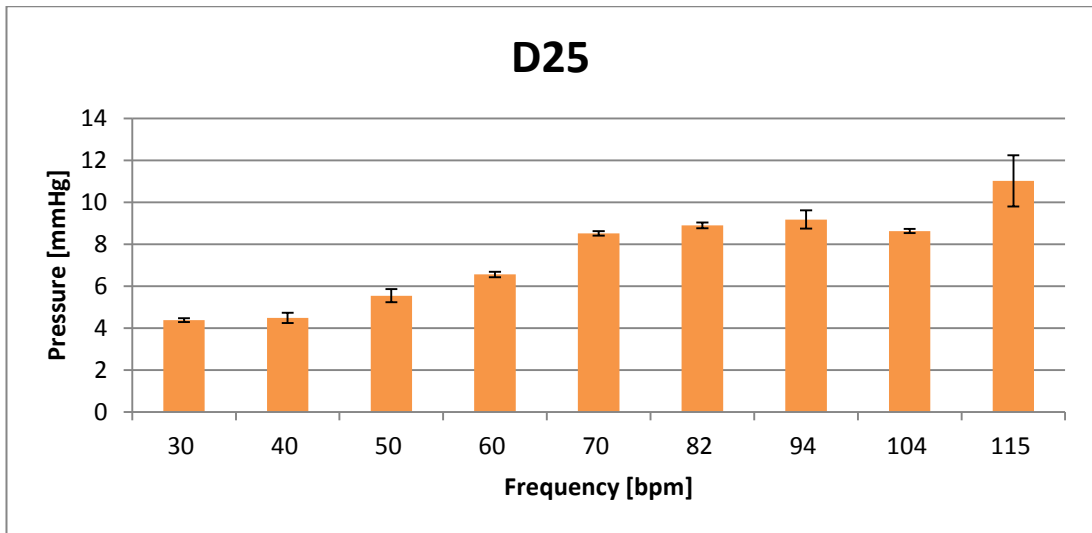


Figure 27: No valve in place - average TPG values represented for 33 mm diameter in bar chart with error bars.

#### 4.2. The CoreValve testing

This part of the experimental work of the project has shown similar behaviour as obtained in previous experiment, although there have been a few differences observed. Firstly, in the collected data, the TPG obtained for each of the three diameters was different. TPG measured with 23 mm diameter ranged from 10 mmHg starting at the lowest heart rate up to around 70 mmHg at the highest heart rate. For 20 mm diameter the TPG was much lower starting with values around 1.5 mmHg at the lowest heart rate up to around 40 mmHg at the highest heart rate. The highest values of TPG were obtained with 16 mm diameter ranging from 40 mmHg at the lowest heart rate up to around 240 mmHg at the highest rate.

The relationship of the higher the frequency is, the higher pressure readings are obtained is valid in these experiments as well. For two of the diameters (23 and 16 mm) a comparison of three frequencies (40, 70 and 104 bpm) is shown below to introduce the differences between the pressure readings expressed by TPG (Figures 25 – 30).

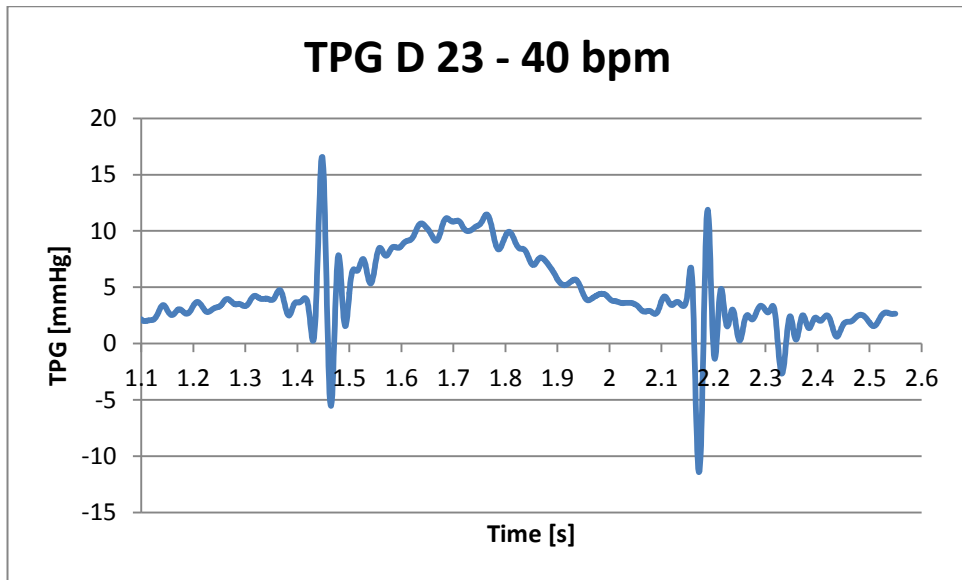


Figure 28: Valve in place – TPG of second cycle measured at 40 bpm, 23 mm diameter.

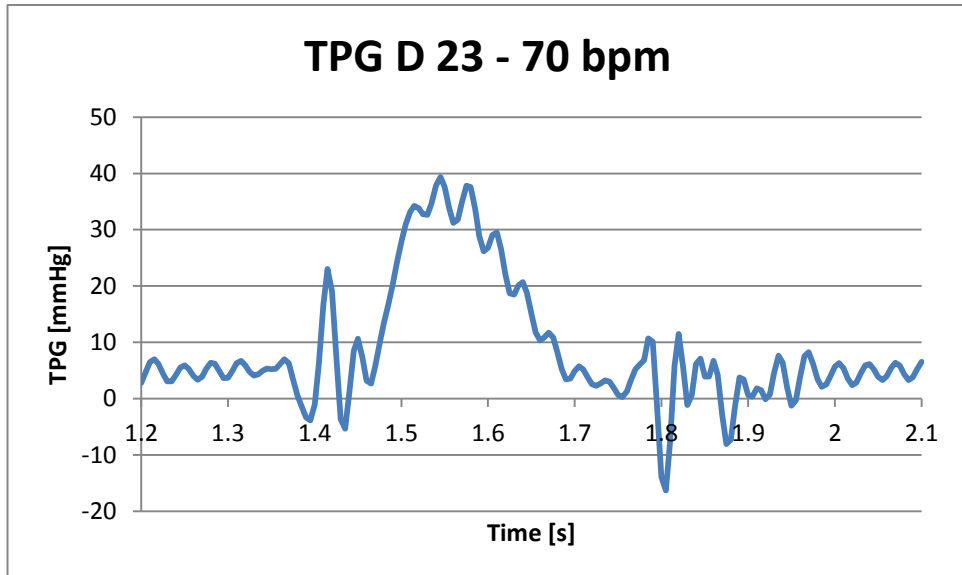


Figure 29: Valve in place – TPG of third cycle measured at 70 bpm, 23 mm diameter.

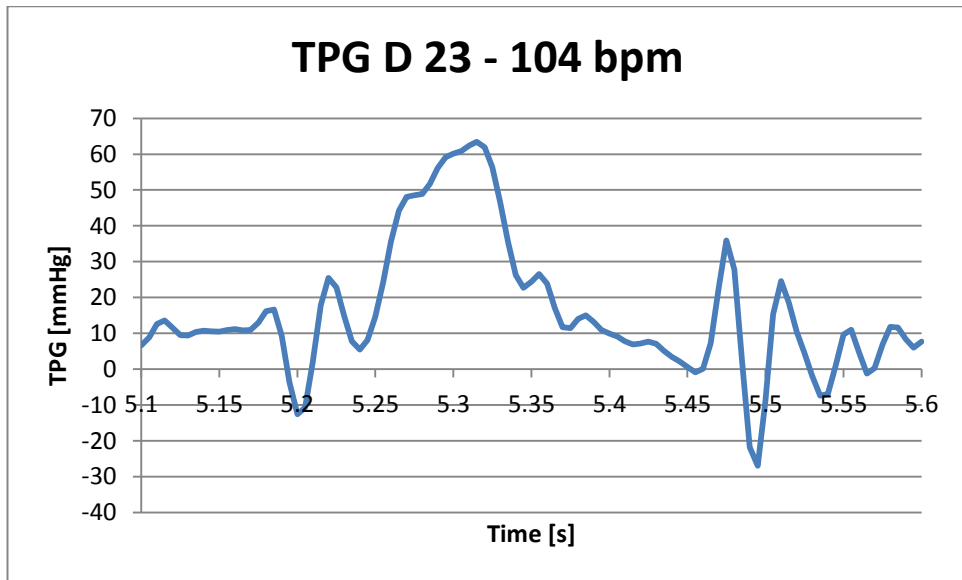


Figure 30: Valve in place – TPG of tenth cycle measured at 104 bpm, 23 mm diameter.

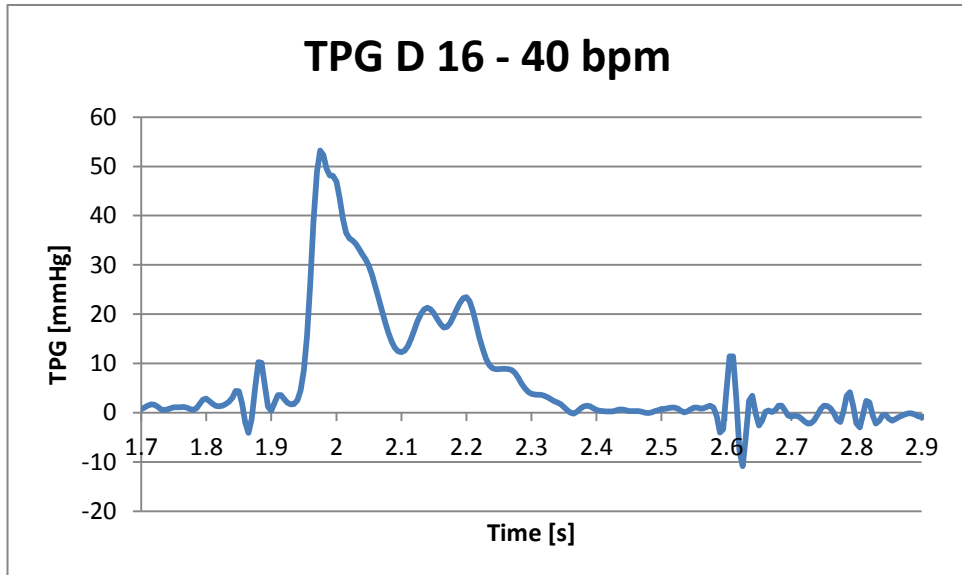


Figure 31: Valve in place – TPG of second cycle measured at 40 bpm, 16 mm diameter.

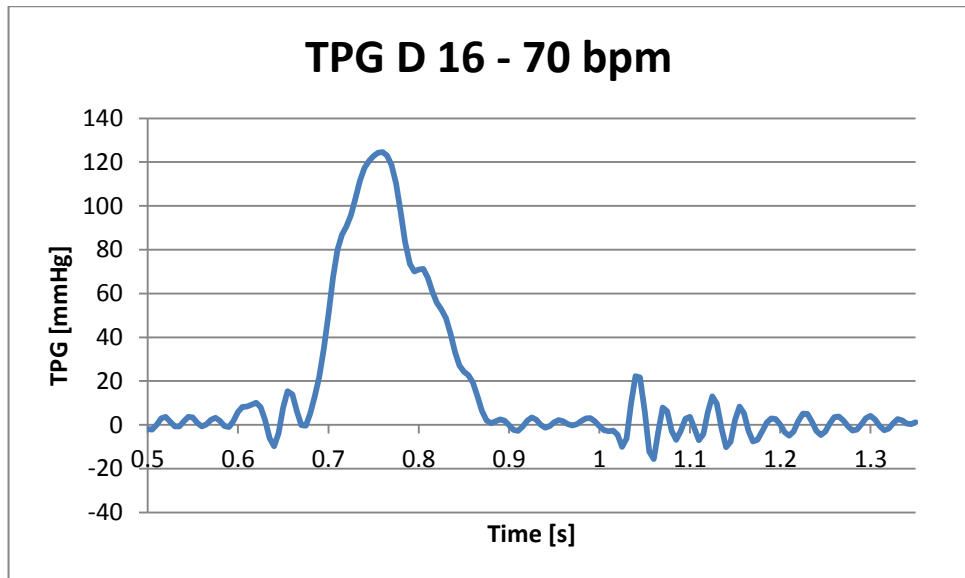


Figure 32: Valve in place – TPG of second cycle measured at 70 bpm, 16 mm diameter.

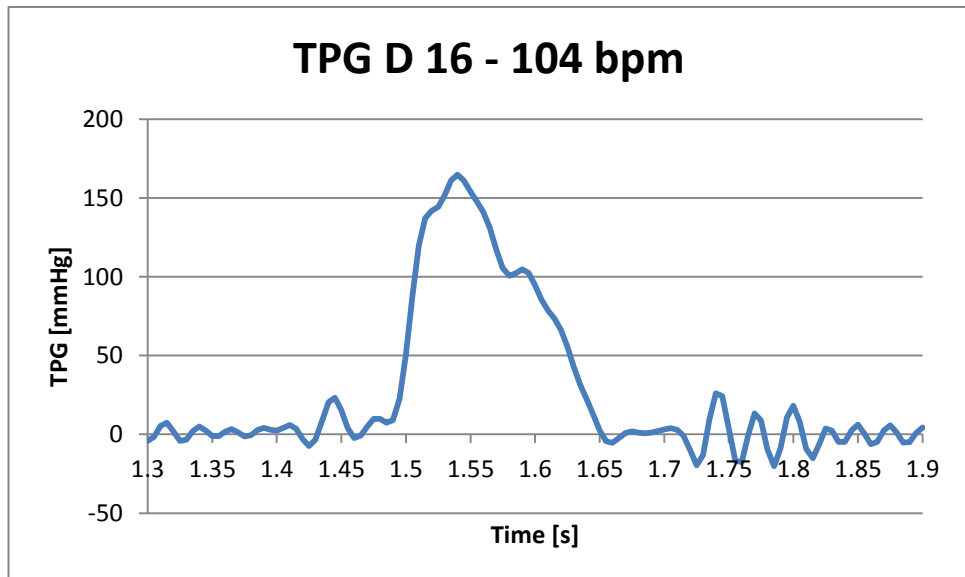


Figure 33: Valve in place – TPG of third cycle measured at 104 bpm, 16 mm diameter.

In Table 4 is shown the average  $\pm$  standard error of the mean (SEM) of 3 maximal values of TPG of each experiment in order to see the pressure changes when the annulus and frequency is increased. Figures 34 - 36 represent data taken from the Table 4 in bar charts with error bars. As it is seen in Figures 34 - 36, the relationship between the frequency and the annulus is fairly linear in each of the diameters except from the 20 mm diameter. Linear behaviour can be observed at 23 and 16 mm diameters with a small deviation at 16 mm where TPG rises at 94 bpm and then declines at 104 bpm. The 20 mm diameter displayed the similar behaviour as 16

mm, with a difference of steeper rise and a decline at exactly the same frequencies as the 16 mm. Values of TPG vary taking all three diameters, having the highest values observed at the smallest 16 mm diameter, and the lowest values observed at 20 mm diameter. The 23 mm diameter displays higher values of TPG than 20 mm diameter.

Table 4: Valve in place - average  $\pm$  standard error of the mean (SEM) of 3 maximal values of TPG, 23, 20 and 16 mm diameters.

	D 23	D 20	D 16
HR	AVG $\pm$ SEM	AVG $\pm$ SEM	AVG $\pm$ SEM
(bpm)	(mmHg)	(mmHg)	(mmHg)
30	15.3 $\pm$ 0.3	1.7 $\pm$ 0.02	39.9 $\pm$ 0.83
40	16.83 $\pm$ 0.12	3.19 $\pm$ 0.01	52.97 $\pm$ 0.27
50	18.88 $\pm$ 0.37	6.47 $\pm$ 0.11	72.61 $\pm$ 0.42
60	26.46 $\pm$ 1.9	10.4 $\pm$ 0.26	97.07 $\pm$ 0.77
70	35.78 $\pm$ 2.45	13.23 $\pm$ 1.5	125.18 $\pm$ 0.07
82	44.08 $\pm$ 2.2	24.1 $\pm$ 2.22	148.9 $\pm$ 1.79
94	54.78 $\pm$ 0.33	39.87 $\pm$ 7.76	172.03 $\pm$ 1.41
104	63.07 $\pm$ 1.38	34.58 $\pm$ 0.49	168.55 $\pm$ 4.39
115	74.11 $\pm$ 1.66	38.91 $\pm$ 1.81	224.6 $\pm$ 9.04

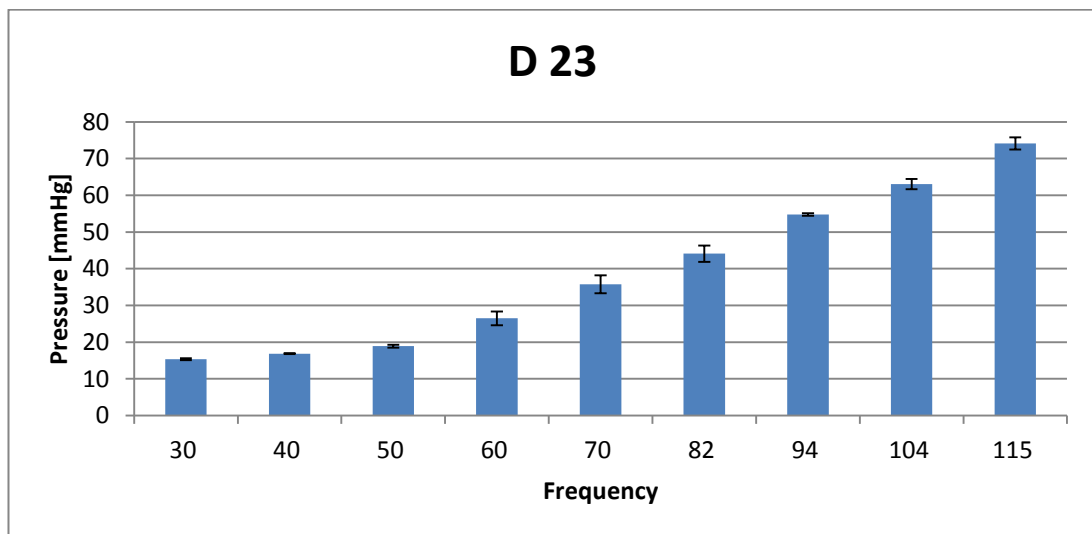


Figure 34: Valve in place - average TPG values represented for 23 mm diameter in bar chart with error bars.

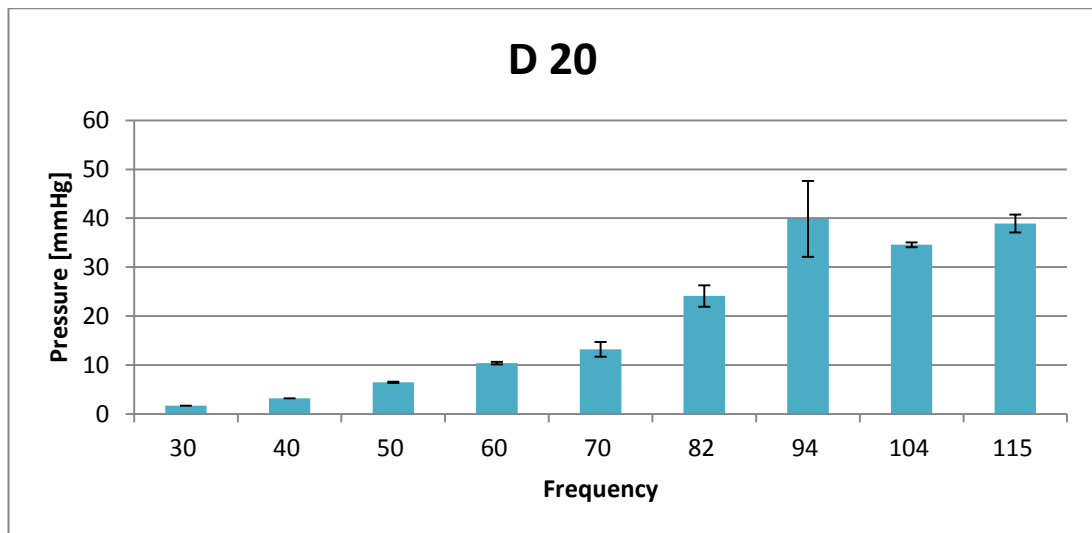


Figure 35: Valve in place - average TPG values represented for 20 mm diameter in bar chart with error bars.

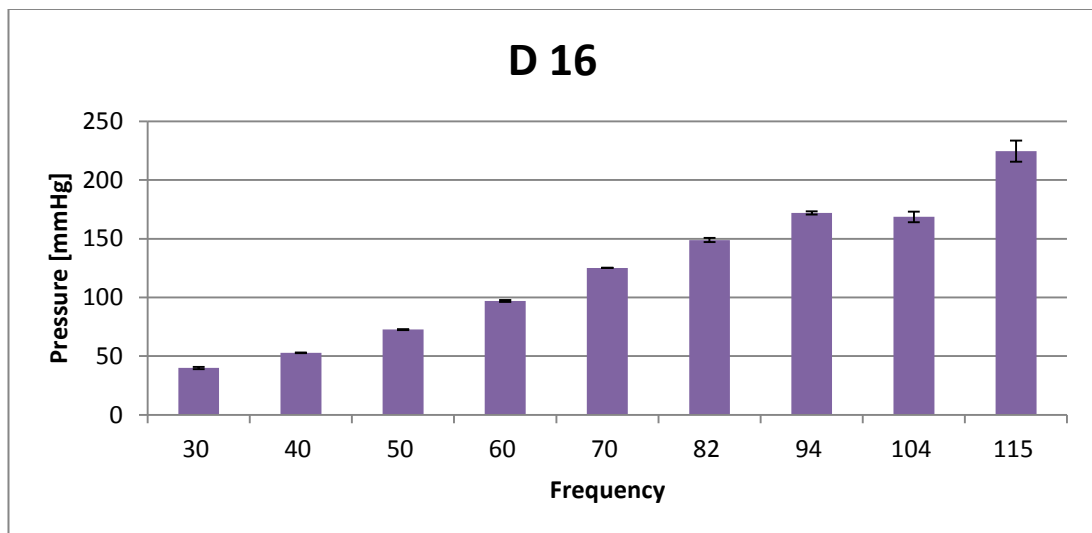


Figure 36: Valve in place - average TPG values represented for 16 mm diameter in bar chart with error bars.

### 4.3. Iris mechanism

#### 4.3.1. Iris mechanism without the CoreValve

A different relationship between the annulus and frequency has been observed in the Iris mechanism without the CoreValve compared to the silicone holder without the valve. The higher the annulus size, the higher TPG displays. Starting with 22 mm diameter, values of TPG were twice as high as values of 9 mm, the smallest diameter in this set of experiments. Ranging from 20 mmHg at the lowest frequency for 22 mm diameter up to around 55 mmHg at the highest frequency. For 16 mm diameter, values of TPG ranged from 15 mmHg at the lowest frequency up to 45 mmHg at the highest frequency. Lastly, for 9 mm

diameter values have been half the values of 22 mm diameter at the lower frequency, but with increasing frequency TPG moved towards the negative values. The relationship higher the frequency is, higher pressure readings are obtained is valid in these experiments as well. For two of the diameters (22 and 16 mm) a comparison of three frequencies (40, 70, 104 bpm) is shown below to introduce the differences between the TPG pressure readings (Figures 32 – 37).

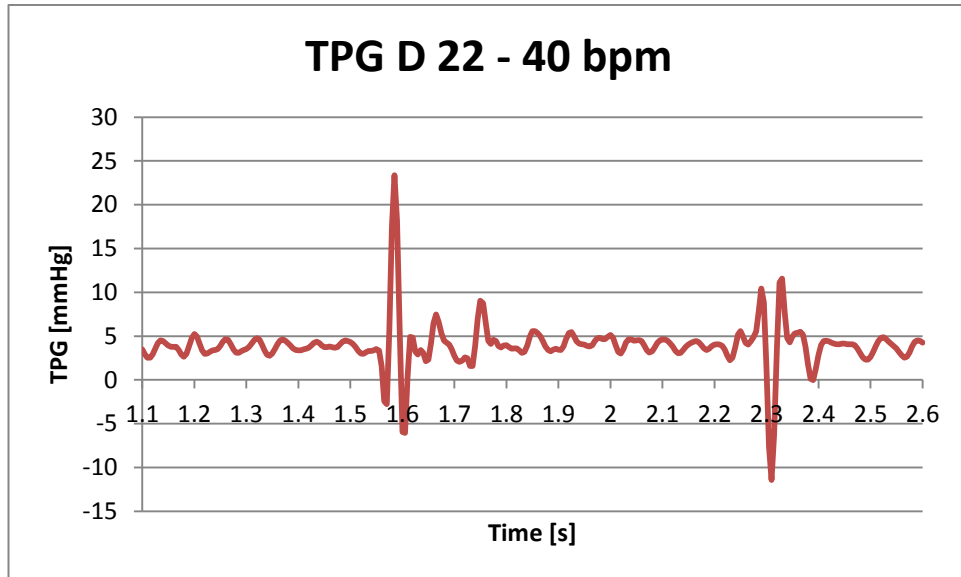


Figure 37: Iris mechanism without the CoreValve – TPG of second cycle measured at 40 bpm, 22 mm diameter.

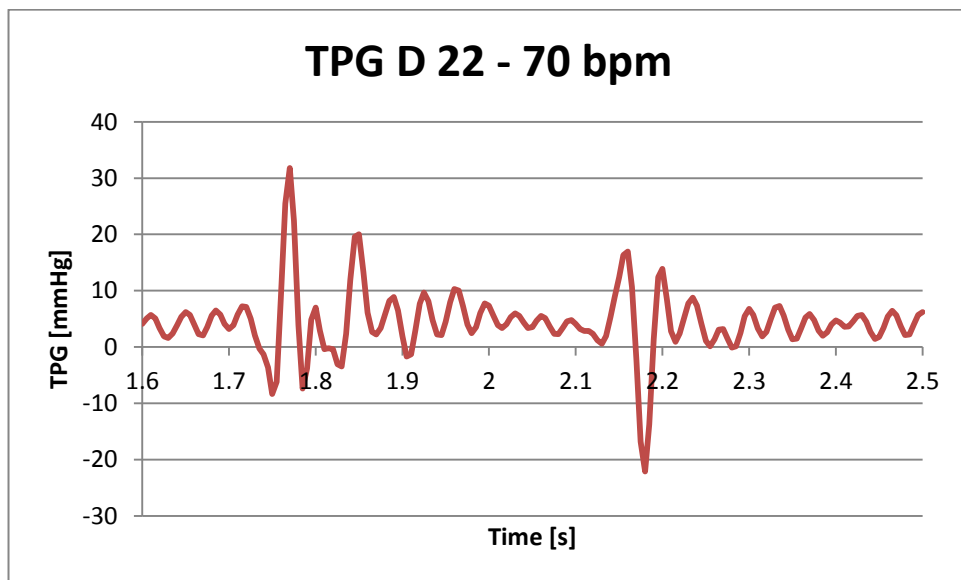


Figure 38: Iris mechanism without the CoreValve – TPG of third cycle measured at 70 bpm, 22 mm diameter.



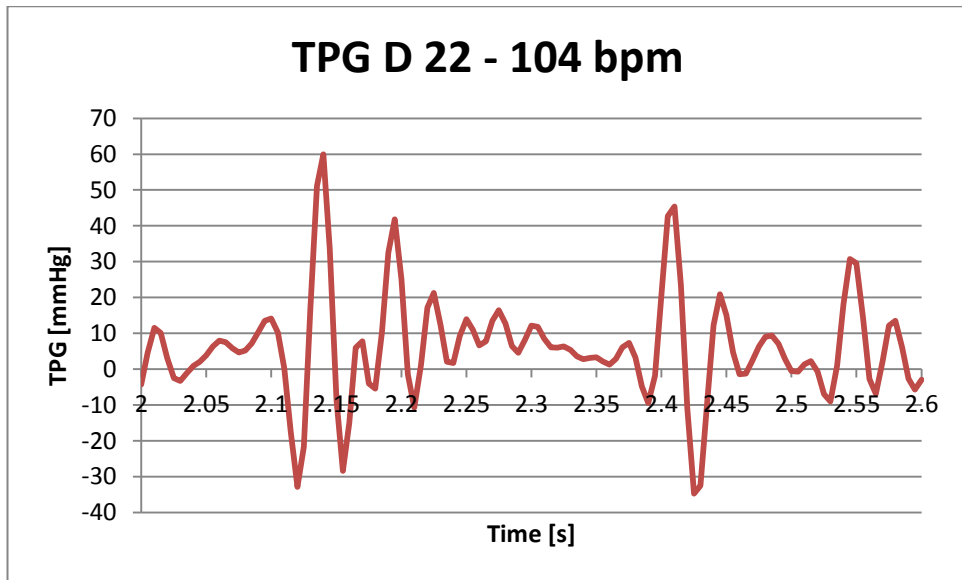


Figure 39: Iris mechanism without the CoreValve – TPG of fourth cycle measured at 104 bpm, 22 mm diameter.

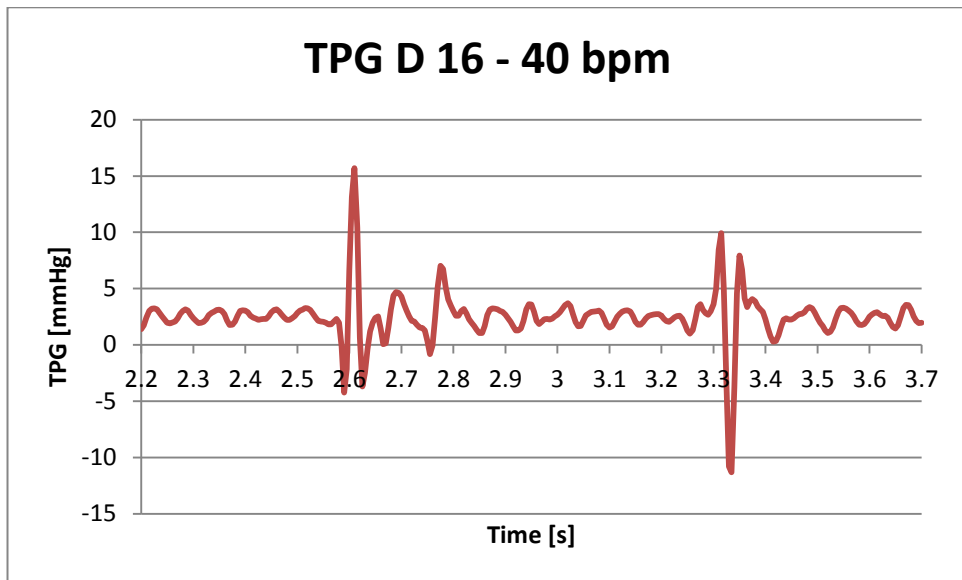


Figure 40: Iris mechanism without the CoreValve – TPG of second cycle measured at 40 bpm, 16 mm diameter.

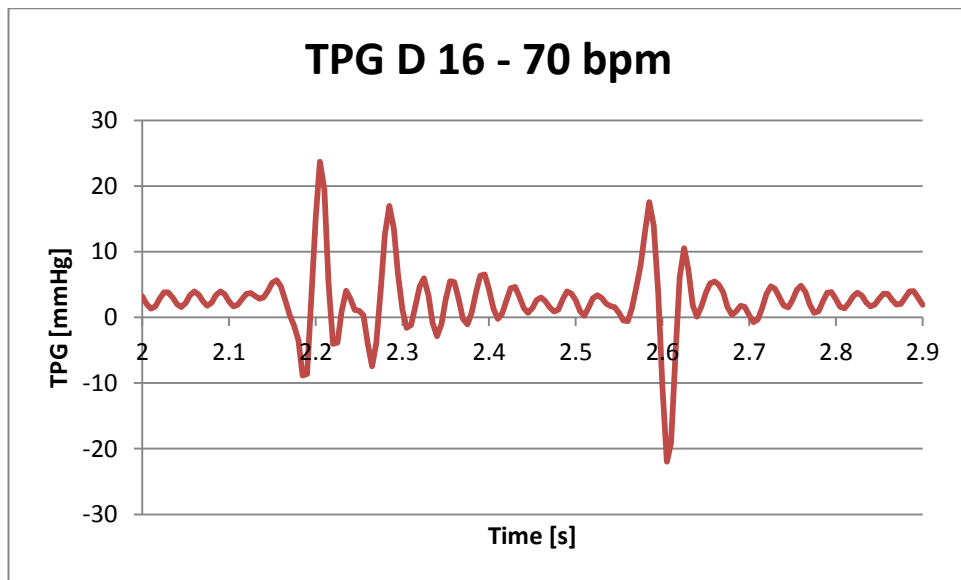


Figure 41: Iris mechanism without the CoreValve – TPG of second cycle measured at 70 bpm, 16 mm diameter.

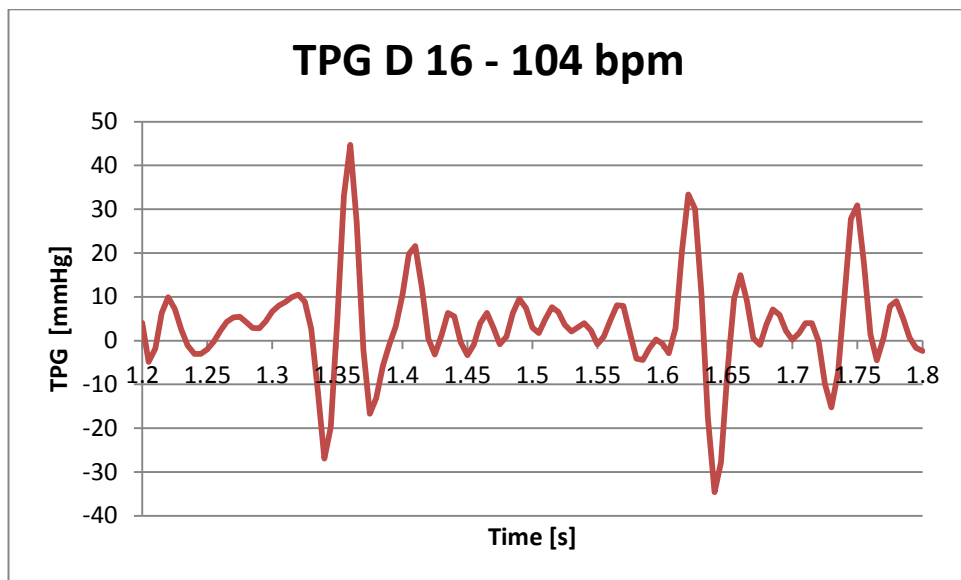


Figure 42: Iris mechanism without the CoreValve – TPG of second cycle measured at 104 bpm, 16 mm diameter.

In Table 5 is shown the average  $\pm$  standard error of the mean (SEM) of 3 maximal values of TPG of each experiment in order to see the pressure changes when annulus and frequency is increased. Figures 43 - 45 represent data taken from the Table 5 in bar charts with error bars. As it is seen in Figures 43 - 45, the relationship between the frequency and the annulus is not linear for each of the diameters. Values of TPG are similar at lower frequencies in comparison to higher frequencies where a sudden step rise in value mostly at 22 mm diameter occurs. At 9 mm

diameter, values are mostly uniform except from 104 bpm frequency where again a steep rise occurs.

**Table 5: Iris mechanism without the CoreValve - average  $\pm$  standard error of the mean (SEM) of 3 maximal values of TPG, 22, 16 and 9 mm diameters.**

	<b>D 22</b>	<b>D 16</b>	<b>D 9</b>
<b>HR</b>	<b>AVG <math>\pm</math> SEM</b>	<b>AVG <math>\pm</math> SEM</b>	<b>AVG <math>\pm</math> SEM</b>
<b>(bpm)</b>	<b>(mmHg)</b>	<b>(mmHg)</b>	<b>(mmHg)</b>
30	20.29 $\pm$ 0.3	14.76 $\pm$ 0.08	9.27 $\pm$ 0.16
40	23.01 $\pm$ 0.05	15.43 $\pm$ 0.21	10.53 $\pm$ 0.11
50	28.27 $\pm$ 0.1	16.79 $\pm$ 0.21	12.14 $\pm$ 0.3
60	30.56 $\pm$ 0.12	22.49 $\pm$ 0.05	12.16 $\pm$ 0.12
70	30.99 $\pm$ 0.48	24.17 $\pm$ 0.31	12.67 $\pm$ 0.48
82	32.27 $\pm$ 3.26	38.20 $\pm$ 0.21	14.23 $\pm$ 0.68
94	54.97 $\pm$ 0.64	40.07 $\pm$ 0.39	14.76 $\pm$ 0.13
104	59.43 $\pm$ 0.88	42.64 $\pm$ 1.31	18.47 $\pm$ 0.15
115	54.52 $\pm$ 1.32	36.46 $\pm$ 10.01	13.53 $\pm$ 0.5

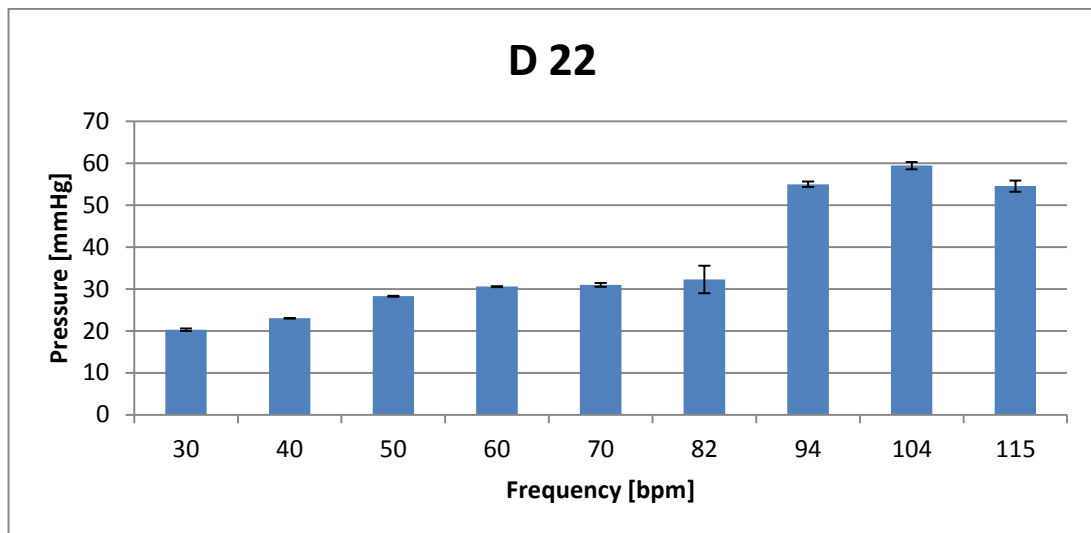


**Figure 43: Iris mechanism without the CoreValve - average TPG values represented for 22 mm diameter in bar chart with error bars.**

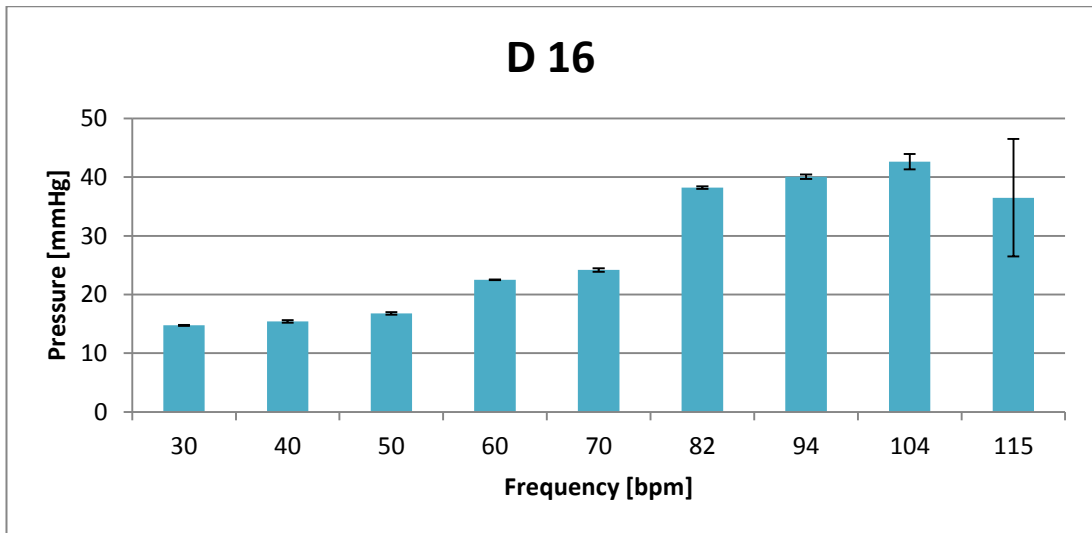


Figure 44: Iris mechanism without the CoreValve - average TPG values represented for 16 mm diameter in bar chart with error bars.

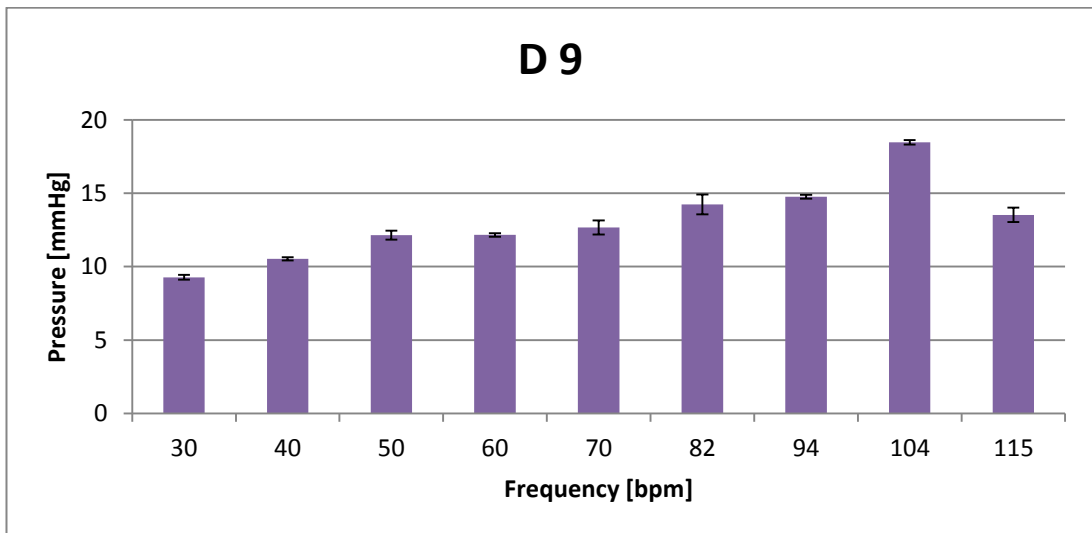


Figure 45: A Iris mechanism without the CoreValve - average TPG values represented for 9 mm diameter in bar chart with error bars.

#### 4.3.2. Iris mechanism with valve

The experiment with the CoreValve held in the Iris mechanism was performed once only due to difficulty of crimping the valve inside the Iris. The TPG obtained during the testing ranged from around 28 mmHg at the lowest frequency up to around 55 mmHg at the highest frequency. These values can be compared against the experiment with the 22 mm Iris diameter without the valve held in place.

The relationship higher the frequency is, higher pressure readings are obtained is valid in these experiments as well. In figures 39 – 41 is shown a comparison of three

frequencies (40, 70 and 104 bpm) to introduce the differences between the pressure readings expressed by TPG.

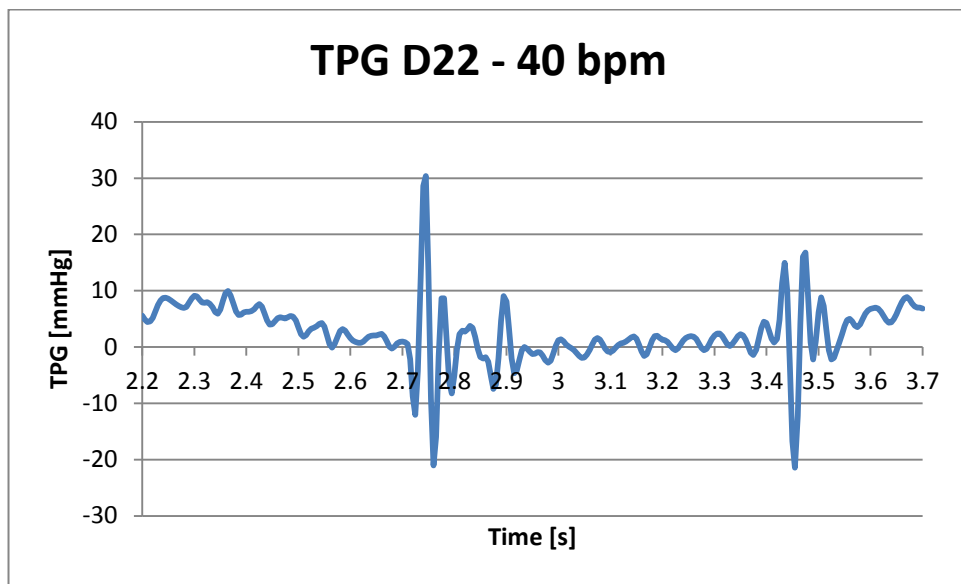


Figure 46: Iris mechanism with the CoreValve – TPG of third cycle measured at 40 bpm, 22 mm diameter.

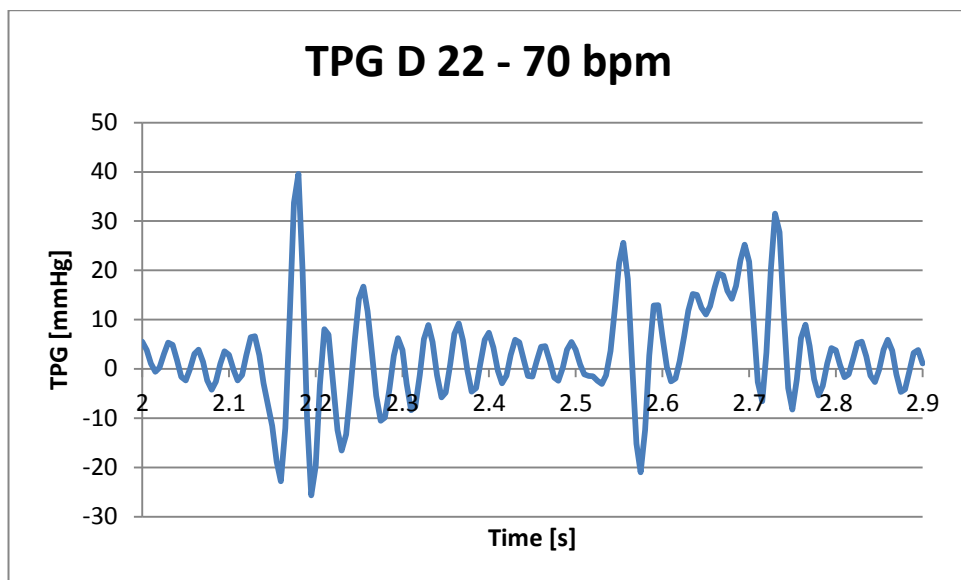


Figure 47: Iris mechanism with the CoreValve – TPG of third cycle measured at 70 bpm, 22 mm diameter.

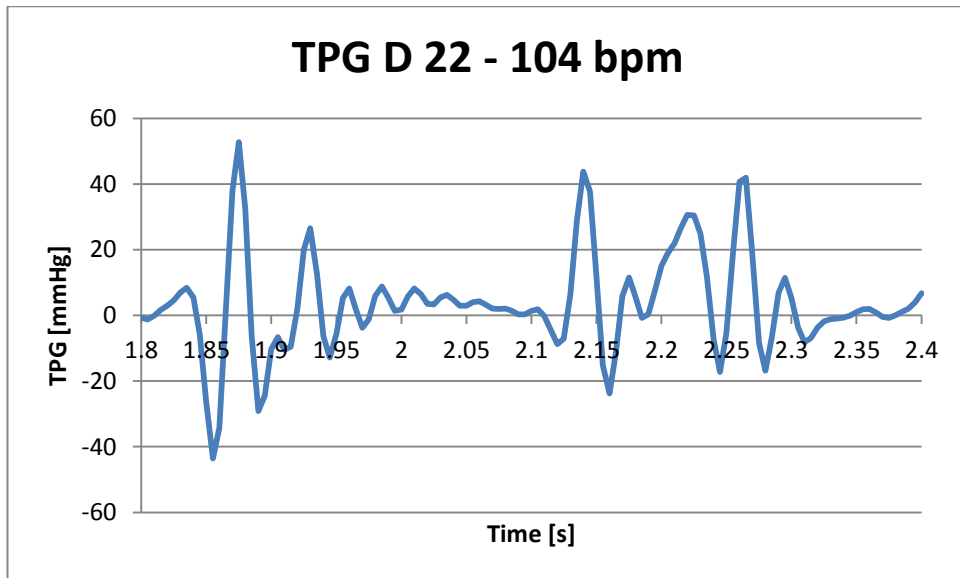


Figure 48: Iris mechanism with the CoreValve – TPG of third cycle measured at 104 bpm, 22 mm diameter.

In Table 6 is shown the average  $\pm$  standard error of the mean (SEM) of 3 maximal values of TPG of each experiment in order to see the pressure changes when the annulus and frequency is increased. Figure 49 represents data taken from the Table 6 in bar charts with error bars. As it is seen in Figure 49, the relationship between the frequency and the annulus is again not linear for 22 mm diameter. Values of TPG are similar at lower frequency in comparison to higher frequency where a sudden steep rise occurs at 82 bpm and then values of TPG again display similar behaviour as at lower frequency.

Table 6: Iris mechanism with the CoreValve - average  $\pm$  standard error of the mean (SEM) of 3 maximal values of TPG for 22 mm diameter.

	<b>D 22</b>
<b>HR</b>	<b>AVG <math>\pm</math> SEM</b>
<b>(bpm)</b>	<b>(mmHg)</b>
30	26.52 $\pm$ 0.52
40	30.92 $\pm$ 0.33
50	37.56 $\pm$ 0.65
60	37.56 $\pm$ 0.65
70	39.87 $\pm$ 0.8
82	52.01 $\pm$ 1.61
94	54.49 $\pm$ 2.08
104	52.28 $\pm$ 0.69
115	53.09 $\pm$ 0.49

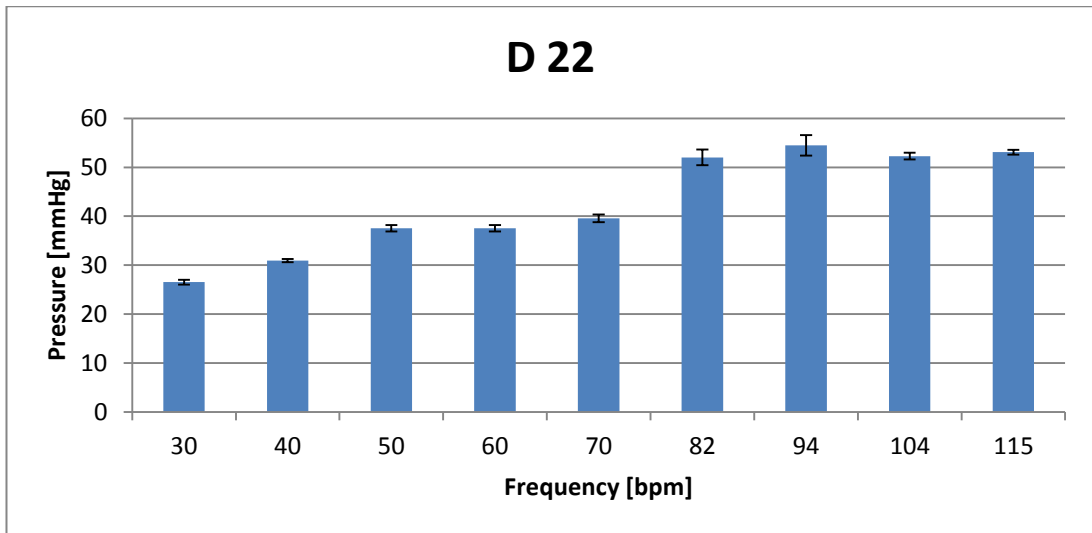


Figure 49: Iris mechanism with the CoreValve - average TPG values represented for 22 mm diameter in bar chart with error bars.

In Figure 50 is shown the TPG difference between the CoreValve placed in the Iris mechanism with 22 mm diameter and the Iris mechanism alone without the CoreValve. At lower frequency, the CoreValve placed in the Iris displayed higher TPG values but with increasing frequency, the values of TPG were slightly higher with the Iris mechanism alone.

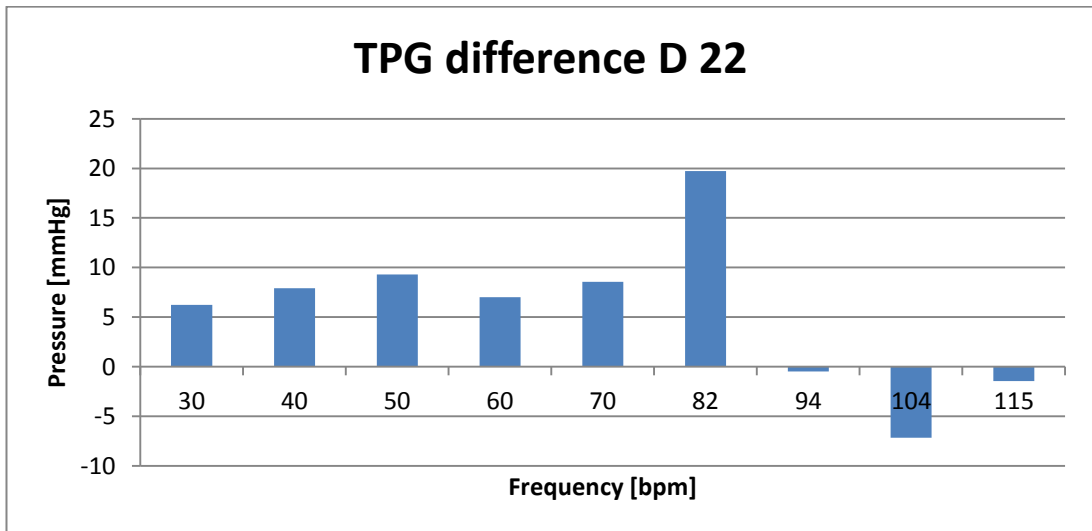


Figure 50: The TPG difference of the CoreValve in the Iris and the Iris alone, 22 mm diameter.

## 5. Discussion

Testing a bioprosthetic heart valve in the pulse duplicator brought several conclusions regarding the pressure distribution through the heart valve. This chapter contains a discussion of each of the experiments results.

### 5.1. Valve not in place

The first set of experiments with the heart valve not in place displayed a general relationship between the frequency and the size of the annulus. The bigger the diameter is, the lower the pressure readings obtained. This is simply because water being pushed through a smaller area needs more force to get through than having a larger area, where there is less resistance to the flow. Therefore at the biggest diameters (33 and 31 mm) the pressure readings were considerably low in comparison to the smaller diameters (27 and 25 mm). The values of TPG were in the range of 0 – 10 mmHg for all of the diameters which shows that there was minimal obstruction through the empty valve holder <sup>30</sup>. With increasing frequency, the pressure readings increased as well due to the water being pushed through the tester, resulting in increased resistance.

### 5.2. The CoreValve testing

The second set of experiments was performed with the heart valve held in place in the valve tester. The relationship between the frequency and the size of the annulus is valid in this case as well, but a few differences in the pressure readings were found. The highest values of TPG are displayed at 16 mm diameter which was the smallest one in this set of tests. Although, the 23 mm diameter was the biggest diameter used in the experiments, it had higher pressure readings than the 20 mm diameter, in average around 20 mmHg higher which displayed a different relationship between the frequency and the size of the annulus. However, higher pressure readings could be caused by a different position of the pressure transducers. Although the pressure ports were checked prior to each set of experiments, if they were not in line with the transducers, it could cause bending which causes decreased diameter of the tubing connecting the transducers, resulting in higher pressure readings. The values of the TPG obtained from these set



of experiments are of higher values, starting from the frequency of 30 bpm where the TPG was around 3 mmHg for 20 mm and around 5 mmHg for 16 mm diameter. With regards to physiological values, the starting TPG value for 16 mm diameter (50 mmHg) represents severe aortic stenosis in the heart<sup>30</sup> which is life threatening to the patient and has to be treated urgently due to the rapid progress of the stenosis. The heart muscle gets weaker and heart cannot provide enough blood supply to the body which can consequently result in the heart failure.<sup>6</sup>

At 16 mm diameter, the CoreValve was crimped with the leaflets held tightly in order to fit in the small diameter. This represented higher pressure readings due to the smaller annulus and increased force that was used to push the solution through the CoreValve. When a disease such as aortic stenosis occurs or insufficient closure of the valve leaflets, it causes regurgitation due to the blood flowing back from the aorta to the left ventricle which places a higher demand on the left ventricle to hold more blood, resulting in weakening the chamber as well as the entire heart.<sup>6</sup>

### **5.3. Iris mechanism**

#### **5.3.1. Iris without the CoreValve**

The third set of experiments was performed on the Iris mechanism without the CoreValve. These experiments showed a totally different relationship between the frequency and the size of the annulus. In previous experiments it has been proved that the higher the annulus, the smaller the TPG obtained. In this case, it is the other way round. The bigger the annulus, the higher the TPG obtained as well as the smaller the annulus is, the lower the TPG obtained. The reason why the relationship is different could be due to the material of the Iris, which was manufactured from ABS plastic material which is a rigid material rather than an elastic material. When blades overlap each other it creates gaps in the mechanism and subsequently water could leak through these gaps. When the Iris is in its fully open position (22 mm) this gap increases and water leaks through the mechanism. Meanwhile when the Iris is in half-closed position (16 and 9 mm), the gap is small enough to prevent water leaking through. During the experiments, it was noticed when the Iris mechanism was used, air bubbles occurred in the system which again leads to the

water leakage. The TPG values of this part of experiments represent moderate aortic stenosis in physiological environment which is between 20 – 39 mmHg.<sup>30</sup> At the 9 mm diameter, as the frequency increased values of TPG were more in the negative bit of graph which means negative values of TPG. It is caused by having a very small diameter where there is not enough pressure to force the water in the system go through the Iris, therefore there is a lot of water coming back from the left ventricular chamber and not reaching the aortic chamber, resulting in high regurgitation.

### 5.3.2. Iris with the CoreValve

The last set of experiments with the Iris was performed with the CoreValve placed on the mechanism. It was possible to test only one diameter due to the difficulty of crimping the valve inside the Iris mechanism and its rigid structure, therefore there were a few comparisons between different diameters and relationship between the frequency and the annulus. However, the relationship between the increasing frequency and increasing pressure readings is valid.

The focus will therefore be more on the CoreValve in the Iris mechanism (22 mm) versus the CoreValve in the tight holder with the silicone mould (23 mm), even though the data collected with the CoreValve in the tight holder displayed higher pressure readings (due to the possible error in the pressure transducers). Regarding the TPG, the CoreValve in the Iris mechanism has a higher TPG (around 30 mmHg at 40 bpm) than in the classic holder (around 17 mmHg at 40 bpm). On the other hand, as the frequency increases, the TPG for the CoreValve in the classic holder increases more (around 60 mmHg at 104 bpm) than for the CoreValve in the Iris mechanism (around 50 mmHg at 104 bpm). Higher TPG values in the classic holder can be caused by water leaking through the edges of the valve in between with the silicone mould when the frequency was increasing and the valve could therefore have migrated during the testing.

Comparing the TPG values of the Iris mechanism with and without the CoreValve at 22 mm diameter brings a conclusion of having higher TPG values for the Iris mechanism with the CoreValve at lower frequency than for the Iris mechanism

alone, meanwhile having higher TPG values for the Iris mechanism itself at higher frequency than for the Iris mechanism with the CoreValve. Higher values of TPG at lower frequencies for the Iris mechanism with the CoreValve could be caused by the valve itself, introducing the higher resistance to the water flow through the mechanism. On the other hand, higher values at higher frequencies for the Iris mechanism alone could be caused by the water leaking through the gaps among the blades of the mechanism.

## 6. Future perspectives

During the period of research for this project many challenges have been discovered that appeared at different stages of the project. Firstly, regarding the design requirements to fulfil the purpose of the expandable mechanism where several design requirements were challenging such as minimal scale on which the expandable holder had to be designed. Valve attachment was one of the key design requirements as well in order to not allow the CoreValve to migrate during the testing. At last, leaking of water was taken into the account to not introduce a different pressure distribution across the system while testing.

Another issue appeared regarding the valve attachment where the special caution to not damage the valve had to be fulfilled. On the other hand, materials of the Iris mechanism and current considerations have to be changed in order to be able to crimp the valve and enable smaller diameters to be tested. This and much more was the part of the project and due to the lack of time, it was not possible to solve all the issues related to this project. Nevertheless, during the research, a few future considerations have been listed in order to improve the expandable holder to be able to expand paediatric heart valves.

### 6.1. Material

The Iris mechanism developed for this project was produced from ABS plastic material (3D printed) which is rigid, not flexible, without sealing which enabled the water to leak through the mechanism. Rubber-like materials are desirable for use in the Iris due to its sealing, non-slipping, flexible and durable properties. This kind of material can be available for 3D printing therefore the use of the material is preferable.

### 6.2. Shape of the Iris

There exist different types of the Iris mechanism, mostly differentiated by the shape of the blades. The previous model was considered alongside the standard Iris mechanism. However, there are better Iris mechanisms that could be deployed in the heart valve testing providing excellent sealing property for the expandable holder. In this case, the blades do not overlap each other which could solve the

leakage problem with the previous model. An example of the mechanism of shutter is shown in Figure 45.

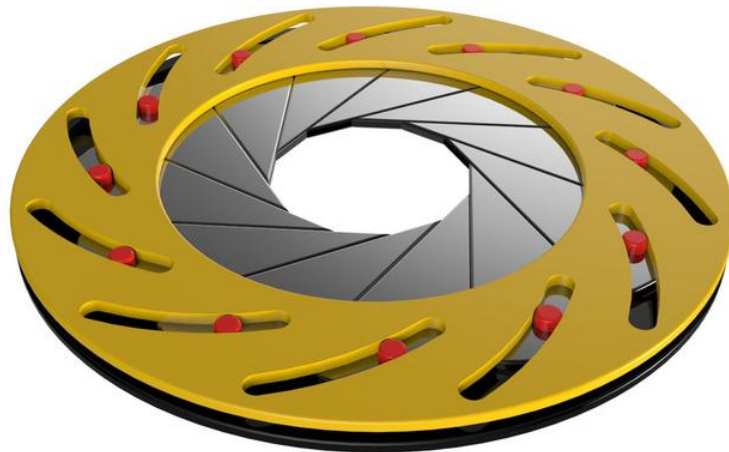


Figure 51: Mechanism of Shutter. An idea for an expandable holder. <sup>31</sup>

### 6.3. Automated mechanism

Right now, the Iris mechanism has to be manually controlled, but as a future perspective it would be highly beneficial if the annulus of the mechanism was crimped or expanded automatically. It would ensure the accuracy of the size of the annulus and at the same time the errors caused by humans would be eliminated. For this fully automated mechanism, a rotary actuator known as a Servomotor could be used which would have precise control over the annulus of the holder. Servomotors work on a close-loop mechanism that uses position feedback to control the motion and the final position. <sup>32</sup>

## 7. Conclusion

The aim of this project was to design an expandable holder for growth compensating paediatric heart valves and perform a set of experiments on the expandable holder in the heart valve tester. Due to the tiny dimensions that paediatric heart valves represent, it brings a big and very complex challenge into the heart valve testing. Speaking about design specifications which have to comply with the expanding property of the holder, material selection, valve attachment, water resistance and many others, the holder has to fulfil all of them listed above. Therefore the Iris mechanism was chosen, having all of the design specifications ticked. As it turned out from the testing stage of the project, the designed Iris mechanism needs to have more improvements to solve the water leakage issue through the mechanism, mostly in terms of material and shape. Another conclusion made regarding the mechanism is to create fully automated self-expanding/crimping Iris to deliver more accuracy in testing and restrict the human factor.

In terms of the heart valve testing, it can be concluded that the higher the annulus, the lower the TPG obtained and opposite, the smaller the annulus, the higher the TPG obtained due to increased resistance. Although the Iris mechanism performed a different pattern, the bigger the annulus, the higher the TPG obtained which was due to water leakage through the valve holder.

The Iris mechanism is a way to go in the heart valve testing especially targeted at paediatrics and constantly changing environment due to growing.

## 8. References

1. Choices N. Congenital heart disease - NHS Choices.  
<http://www.nhs.uk/conditions/Congenital-heart-disease/Pages/Introduction.aspx>. Accessed July 10, 2015.
2. Martini F, Nath JL, Bartholomew EF. *Fundamentals of Anatomy and Physiology*. Benjamin Cummings; 2012.  
<https://books.google.com/books?id=yN9xtQAACAAJ&pgis=1>. Accessed July 9, 2015.
3. Heart.  
<http://www.kidport.com/reflib/science/humanbody/cardiovascular/Heart.htm>. Accessed July 9, 2015.
4. Chambers and the valves of the heart - Mayo Clinic.  
<http://www.mayoclinic.org/chambers-and-valves-of-the-heart/img-20007497>. Accessed July 9, 2015.
5. Thubrikar MJ. *The Aortic Valve*. Taylor & Francis; 1989.  
[https://books.google.co.uk/books/about/The\\_Aortic\\_Valve.html?id=XH826W9s\\_wwC&pgis=1](https://books.google.co.uk/books/about/The_Aortic_Valve.html?id=XH826W9s_wwC&pgis=1). Accessed June 5, 2015.
6. Iaizzo PA, ed. *Handbook of Cardiac Anatomy, Physiology, and Devices*. Totowa, NJ: Humana Press; 2009. doi:10.1007/978-1-60327-372-5.
7. *Pathobiology of Human Disease: A Dynamic Encyclopedia of Disease Mechanisms*. Elsevier Science; 2014.  
<https://books.google.com/books?id=uQB0AwAAQBAJ&pgis=1>. Accessed July 9, 2015.
8. Williams TH, Jew JY. Is the mitral valve passive flap theory overstated? An active valve is hypothesized. *Med Hypotheses*. 2004;62(4):605-611. doi:10.1016/j.mehy.2003.12.001.
9. URGO MEDICAL : The venous system within the cardiovascular system.  
<http://www.urgo.co.uk/260-the-venous-system-within-the-cardiovascular-system>. Accessed July 9, 2015.
10. Hinton RB, Yutzey KE. Heart valve structure and function in development and disease. *Annu Rev Physiol*. 2011;73:29-46. doi:10.1146/annurev-physiol-012110-142145.
11. Misfeld M, Sievers H-H. Heart valve macro- and microstructure. *Philos Trans R Soc B Biol Sci*. 2007;362(1484):1421-1436. doi:10.1098/rstb.2007.2125.

12. Heart Valve Replacment.  
[http://www.womensheart.org/content/heartsurgery/heart\\_valve\\_replacment.aspx](http://www.womensheart.org/content/heartsurgery/heart_valve_replacment.aspx). Accessed July 9, 2015.
13. Chordae Tendinae : Mitral Valve Repair Reference Center.  
<http://www.mitralvalverepair.org/content/view/55/>. Accessed July 9, 2015.
14. Dasi LP, Simon H a., Sucusky P, Yoganathan AP. Fluid mechanics of artificial heart valves. *Clin Exp Pharmacol Physiol*. 2009;36(2):225-237. doi:10.1111/j.1440-1681.2008.05099.x.
15. Rozeik M, Wheatley D, Gourlay T. The aortic valve: structure, complications and implications for transcatheter aortic valve replacement. *Perfusion*. 2014;29(4):285-300. doi:10.1177/0267659114521650.
16. Types of Congenital Heart Defects - NHLBI, NIH.  
<http://www.nhlbi.nih.gov/health/health-topics/topics/chd/types>. Accessed July 10, 2015.
17. Choices N. Aortic valve replacement - Why it is necessary - NHS Choices.  
<http://www.nhs.uk/Conditions/Aorticvalverepacement/Pages/Whyitisnecessary.aspx>. Accessed July 10, 2015.
18. BAVgenetics: dedicated to discovering the genetic causes of bicuspid aortic valve disease and associated aortic disease. <http://bav-genetics.org/>. Accessed July 10, 2015.
19. Melody® Transcatheter Pulmonary Valve (TPV) Therapy by Medtronic treats congenital heart disease and failing heart valves. Explore heart valve replacement treatments like TPV, balloon angioplasty, or conduit replacement. <http://www.medtronic.com/melody/patient/therapy.html>. Accessed July 10, 2015.
20. Melody® TPV Therapy and Ensemble® Transcatheter Valve Delivery | Medtronic US. <http://www.medtronic.com/melody/melody-system.html>. Accessed July 10, 2015.
21. Boston Childrens surgeons pilot expandable prosthetic valves for congenital heart disease patients | Boston Children's Hospital.  
<http://www.childrenshospital.org/news-and-events/2012/october-2012/boston-childrens-surgeons-pilot-expandable-prosthetic-valves-for-congenital-heart-disease-patients>. Accessed July 10, 2015.
22. Henaine R, Roubertie F, Vergnat M, Ninet J. Valve replacement in children: A challenge for a whole life. *Arch Cardiovasc Dis*. 2012;105(10):517-528. doi:10.1016/j.acvd.2012.02.013.



23. Alsoufi B. Aortic valve replacement in children: Options and outcomes. *J Saudi Hear Assoc.* 2014;26(1):33-41. doi:10.1016/j.jsha.2013.11.003.
24. E-echocardiography. <https://e-echocardiography.com/page/page.php?UID=1867001>. Accessed July 29, 2015.
25. Sharland GK, Allan LD. Normal fetal cardiac measurements derived by cross-sectional echocardiography. *Ultrasound Obstet Gynecol.* 1992;2(3):175-181. doi:10.1046/j.1469-0705.1992.02030175.x.
26. Rubber-Like Materials for 3D Printing | Stratasys. <http://www.stratasys.com/materials/polyjet/rubber-like/>. Accessed July 29, 2015.
27. HT-020-035SS - 20mm-35mm Diameter Worm Drive Hose Clip Hi-Torque Stainless Steel (Natural). <http://www.protex.com/HT-020-035SS-20mm-35mm-diameter-worm-drive-hose-clip-hi-torque-stainless-steel-natural>. Accessed July 23, 2015.
28. max rigged iris mechanism. <http://www.turbosquid.com/3d-models/max-rigged-iris-mechanism/757651>. Accessed July 30, 2015.
29. Simulated Blood Products: 10% Glycerol in water may NOT be “One Size Fits All” | William Labs. <http://williamlabs.com/aabb-topics-guidelines/simulated-blood-products-10-glycerol-in-water-is-not-one-size-fits-all/>. Accessed July 30, 2015.
30. Aortic Valve Disease. <http://www.clevelandclinicmeded.com/medicalpubs/diseasemanagement/cardiology/aortic-valve-disease/Default.htm>. Accessed August 11, 2015.
31. Mechanism of Shutter - KeyShot, SOLIDWORKS, Other - 3D CAD model - GrabCAD. <https://grabcad.com/library/mechanism-of-shutter-1>. Accessed July 23, 2015.
32. How Servo Motors Work. <http://www.jameco.com/jameco/workshop/howitworks/how-servo-motors-work.html>. Accessed August 11, 2015.